FRONT PAGE

# PROJECT FINAL REPORT

**Grant Agreement number: PIEF-GA-2011-298927**

**Project acronym: PFMS**

**Project title: Pattern Formation in Microorganism Suspensions: Shear and Confinement**

**Funding Scheme: Intra-European Fellowships (IEF)**

**Period covered: from 01/09/2012 to 08/10/2013**

**Name of the scientific representative of the project's co-ordinator[1], Title and Organisation:**

**Prof. Raymond E. Goldstein,**

**Schlumberger Professor of Complex Physical Systems**

**Tel: +44 1223 337908**

**Fax: +44 1223 765900**

**E-mail: R.E.Goldstein@damtp.cam.ac.uk**

**Project website[2] address:**

http://www.damtp.cam.ac.uk/user/yh343/

[1] Usually the contact person of the coordinator as specified in Art. 8.1. of the Grant Agreement.

[2] The home page of the website should contain the generic European flag and the FP7 logo which are available in electronic format at the Europa website (logo of the European flag: http://europa.eu/abc/symbols/emblem/index_en.htm logo of the 7th FP: http://ec.europa.eu/research/fp7/index_en.cfm?pg=logos). The area of activity of the project should also be mentioned.

## 4.1 Final Publishable Summary Report

### • An executive summary (not exceeding 1page)

This report summarizes research activities and academic achievement of the fellow, Dr. Yongyun Hwang, from 1st September 2012 to 8th October 2013, by carrying out the project 'Pattern formation in microorganism suspensions: shear and confinement'. The project leads the fellow to a permanent academic position, thus it is terminated in the middle of progress.

The research activities for the period have been focused on understanding the role of external shear flow in a collective behaviour of swimming gyrotactic microorganism suspensions by performing mathematical and computational analysis of the state-of-the-art continuum model. A summary of the research activities is as follows:

1. Gaining fundamental understanding and prediction on the role of uniform shear in bioconvection pattern in gyrotactic swimming microorganism suspensions;
2. Elucidating the physical mechanisms of the blip instability observed in downflowing gyrotactic swimming microorganism suspensions (currently in progress)

The research activities leads the fellow to the following academic achievement:

1. Two scientific papers are expected in peer-review journals, one of which is already accepted and the other is currently in preparation. In particular, the first paper will appear in the Journal of Fluid Mechanics, the leading journal in fluid mechanics,
2. Attended four international and domestic conferences to interact with internationally renowned academics in the field,
3. Gave four invited talks at academic institutions such as University of York, Imperial College London, University of Manchester, and University of Cambridge,
4. Have been established research activities in the field of biological fluid mechanics and have been developing collaboration with academics at University of York (M. A. Bees), University of Oxford (Dr. W. M. Durham) and University of Cambridge (Dr. O. A. Croze).
5. Gained a permanent academic position at Imperial College London.

### • A summary description of project context and objectives (not exceeding 4 pages)

Microorganisms are present in almost every part of temperate aqueous environments, and play a critical role in pathogenic infection, digestion, reproduction, and food chains in the oceans. They are also an important source of alternative fuel which can be harvested in bioreactors. Therefore, understanding and modelling their motility, collective dynamics, and interaction with the environment are crucial to overcome important challenges of today such as collapse of ecological systems, global warming, environmental pollution, and energy depletion. However, our understanding of the dynamics of the swimming microorganisms remains elusive particularly for their collective behaviour, which highly interacts with the surrounding fluid flows. Collective behaviors of swimming

microorganisms have been observed in a number of experiments, and their fundamental mechanisms have often been found to originate from the interaction of microorganism motility with surrounding fluids. This interaction often involves instability of the suspension, and it eventually leads to large-scale collective behavior. In this work, we consider the collective dynamics in a gyrotactic swimming microorganism suspension, bioconvection, and study how hydrodynamic shear affects the collective dynamics of swimming microorganisms.

Bioconvection is a pattern forming motion observed in shallow suspensions of cells which swim upward (against gravity). The up-swimming cells accumulate at the top and form a layer with dense population. If the cell concentration is great enough, the heavy layer at the top results in gravitational overturning, leading to a convection pattern analogous to that in Rayleigh-Bénard convection. Childress and coworkers [6] developed a mathematical model in which they took the vertical drift by the up-swimming of cells into account, and showed the appearance of the gravitational instability.

The mechanism by which the individual cells swim upward is often governed by biased swimming of the given cell species in response to external stimuli such as gravity, light, and chemicals (i.e. *taxes*) [34, 17, 29]. Of particular interest to the present study are algal cells such as *C. Nivalis* and *Dunaliella*, and colonies such as *Volvox*, that respond to gravity in the absence of flow. These cells are structurally featured to be bottom-heavy: their center of mass is located behind the center of buoyancy. Therefore, when a cell of this type is not oriented vertically, the bottom heaviness results in a gravitational torque which changes the cell's swimming direction to align with the vertical. In a moving fluid, a viscous torque originating from the shear is also applied to the cell. Therefore, in this case, the cell experiences both gravitational and viscous torques, and the swimming direction is determined by the balance between them. This process, known as 'gyrotaxis', was proposed and demonstrated by Kessler in a series of pioneering experiments [24, 25, 26]. In particular, he showed that, in the presence of a downward shear flow, the cells swim toward the region of most rapid downflow as a result of gyrotaxis.

The gyrotactic nature of the cell has been found to cause instability even in a uniform suspension, which does not exhibit the instability mechanism of gravitational overturning. Imagine a uniform suspension in which natural fluctuations create a 'blob' of cells denser than its surroundings. The blob will sink relative to its surroundings, and will create a downward shear flow in its wake. Owing to the gyrotaxis, other cells in the surroundings swim toward the blob and its wake, where the downflow is most rapid. The blob therefore becomes denser and creates more rapid downflow, resulting in instability of the suspension. The fluid motion resulting from this instability mechanism appears in the form of a bottom-standing plume, which is typically observed in relatively deep suspensions ($d > 1cm$ where $d$ is the depth of the suspension) [26, 34]. Pedley and coworkers [31] analysed this instability by describing the swimming of the cell in a deterministic manner with a prescribed translational diffusivity to take randomness in the cell motion into account. This is later further extended with an improved description on the cell's random behaviour observed to resemble a random walk [33]. They introduced a quasi-steady Fokker-Planck equation for the probability density function (pdf) of the cells' orientation, which allowed them to calculate the mean cell orientation and the related translational diffusivity in a statistical manner. In that study, the effect of the cells' swimming on the fluid motions was also assessed although it was found to be negligible for the gyrotactic instability. Recently, Pedley further extended this model by allowing the pdf of cell orientation to vary over time and space as well as its swimming direction [30]. The model was designed to be more general than the early one, so that it can be applied to other cells such as bacteria and spermatozoa. Thus, it exhibits not only the gyrotactic instability but also the instability observed in dense bacterial suspensions and shown to be a consequence of the intrinsic stresslet of swimming cells [41, 9, 37, 38].

While the early studies focused mostly on suspensions in stationary fluid, many swimming microorganisms in aqueous environments are exposed to shear flow; for gyrotactic cells, in particular, the shear plays a critical role in their swimming behaviour. As mentioned, the swimming direction of a gyrotactic cell is determined by the balance between gravitational and viscous torques. When the shear rate is not large, the balance simply makes the cell's swimming direction tilt towards that of the shear. With an increase of the shear rate, the swimming direction is tilted more and more and the effect of the viscous torque gradually becomes dominant. When the shear rate is large enough, the viscous torque dominates over the gravitational one. In this case, the swimming direction of the cell becomes unsteady and changes periodically in time [32, 34], similarly to that of a passive particle in a shear flow [20]. Owing to this behaviour, gyrotactic cells in a strong shear flow tumble and exhibit greatly reduced up-swimming velocity on average. As a consequence, dispersion of the cells in the vertical direction is significantly disturbed, leading to the formation of layers of cells in regions of strong shear [11, 19].

In spite of the interesting behaviour of gyrotactic cells under shear flows, there have been few studies of how shear affects the bioconvection pattern. Only recently, this issue has been addressed in an experimental study by [7], in which they examined the effect of a cross flow on a bioconvection pattern. They showed that the cross flow tilts the convection pattern in the direction of the shear. Also, with an increase of the flow rate, they observed an increase in the wavelength of the convection pattern. In particular, when the cell concentration is relatively low, the convection pattern was shown to be nearly extinguished. In spite of this interesting observation, no theoretical study which examines the role of shear in bioconvection is currently available, and thus no sound explanation of the observation has yet been provided.

The purpose of the present study is therefore to understand how shear affects the instability of a shallow suspension of gyrotactic cells within a theoretical and computational framework. To gain fundamental understanding of the role of shear, we consider a very simple flow configuration in which a uniform horizontal shear is imposed in a channel by moving the upper and lower walls in opposite directions: i.e. a plane Couette flow (see also figure 1). The mathematical description of the suspension follows [30] and a few approximations are then made. Particular emphasis in the analysis is given to understanding the physical mechanisms by which the shear affects bioconvective instability. From this perspective, we carefully reexamine the physical mechanisms of bioconvection, and this enables us to find an additional physical mechanism for the instability that originates from negative cross diffusion in the unstably stratified circumstances. We will see that shear orchestrates these three instability mechanisms in a different manner, resulting in intricate competition dynamics between them.

## • A description of the main S & T results/foregrounds (not exceeding 25 pages)

### Problem formulation

- *Equations of motion*

We consider a fluid flow with density $\rho$ and kinematic viscosity $\nu$ in which gyrotactic cells are suspended with gravity heading downward. We denote $x^*$, $y^*$, and $z^*$ as the streamwise, wall-normal, and spanwise directions, respectively, and $t^*$ is the time (the superscript $^*$ indicates dimensional variables). The suspension is bounded by two infinitely long and wide parallel walls, respectively

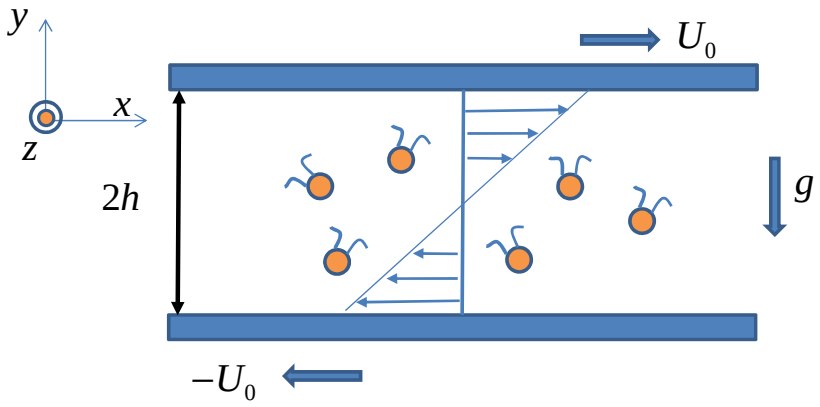


Figure 1: Schematic diagram of flow configuration in the present study.

located at $y^* = \pm h$, and they are set to move in opposite directions with velocity $U_0^*$. The fluid motion is described by the following equations:

$$\nabla^* \cdot \mathbf{u}^* = 0, \tag{1}$$

$$\frac{\partial \mathbf{u}^*}{\partial t^*} + (\mathbf{u}^* \cdot \nabla^*)\mathbf{u}^* = -\frac{1}{\rho}\nabla^* p^* + \nu \nabla^2 \mathbf{u}^* - n^* \upsilon g' \mathbf{j} + \nabla^* \cdot \Sigma_p^*, \tag{2}$$

Here, $\mathbf{u}^*$ is the velocity, $p^*$ the pressure, $n^*$ the cell number density, $g' = g\Delta\rho/\rho$ the reduced gravity ($\Delta\rho$ is the density difference between cell and fluid, and $g$ the gravitational acceleration), $\upsilon$ the volume of a single cell, and $\mathbf{\Sigma}_p^*$ the additional stress term caused by the presence of swimming cells in the suspension. This term $\mathbf{\Sigma}_p^*$ was first analysed by [33], in which they showed that it is dominated by the stresslets associated with the locomotion of the cells. Recent analyses have shown that this term actually plays a cruical role in generating an instability in dense suspensions of 'pusher'-type swimmers (e.g. bacteria and spermatozoa), which generate thrust by pushing the fluid behind the cell body [41, 37, 38, 30]. However, in the present study, we will consider only 'puller'-type swimmers (e.g. *Chlamydomonas*), which swim by pulling fluid from the front to the back. In this case, the cell-stress term is not in general responsible for generating such an instability [37, 38, 30]. Also, the instability in bioconvection is typically observed in dilute suspensions (typically less than 1% of cell concentration), in which this term was shown to be negligible [33]. Therefore, this term will be neglected throughout the present study.

For the spatial distribution and orientation of the cells in the suspension, we consider a Smoluchowski equation which describes a conservation law for the probability density distribution as a function of spatial position $\mathbf{x}^* = (x^*, y^*, z^*)$ and of the unit vector in the swimming direction, $\mathbf{e} = (e_1, e_2, e_3)$:

$$\frac{\partial \Psi^*}{\partial t^*} + \nabla^* \cdot (\frac{d\mathbf{x}^*}{dt^*}\Psi^*) + \nabla_e \cdot (\frac{d\mathbf{e}}{dt^*}\Psi^*) = 0, \tag{3a}$$

where

$$\frac{d\mathbf{x}^*}{dt^*} = \mathbf{u}^* + V_c^* \mathbf{e} - V_s^* \mathbf{j} - \mathbf{D}_T^* \cdot \nabla^*(ln\Psi^*), \tag{3b}$$

$$\frac{d\mathbf{e}}{dt^*} = \frac{1}{2B}[\mathbf{j} - (\mathbf{j}\cdot\mathbf{e})\mathbf{e}] + \frac{1}{2}\mathbf{\Omega}^* \wedge \mathbf{e} + \alpha_0 \mathbf{e}\cdot\mathbf{E}^*\cdot(\mathbf{I}^* - \mathbf{ee}) - D_R^* \nabla_e(ln\Psi^*). \tag{3c}$$

Here, $\Psi^*(\mathbf{x}^*, \mathbf{e}, t^*)$ is the probability density distribution function, $\mathbf{i}$, $\mathbf{j}$, and $\mathbf{k}$ are respectively unit vectors in the streamwise, wall-normal and spanwise directions, $V_c^*$ is the cell swimming speed, $V_s^*$

the cell sedimentation speed, $\mathbf{D}_T^*$ the translational diffusivity tensor, $B = \nu\alpha_\perp/2gl$ is the gyrotactic time scale ($l$ is the center of gravity offset), $\mathbf{\Omega}^*$ the vorticity, $\mathbf{E}^*$ the strain rate tensor, and $D_R^*$ the rotational diffusivity. Here, $\alpha_0$ in (3c) and $\alpha_\perp$ in the definition of $B$ are constants given by geometry of the cell: for example, $\alpha_0 = 0.31$ and $\alpha_\perp = 6.8$ for *C. Nivalis* [31]. In the present study, we assume for simplicity that the cell is completely spherical, giving $\alpha_0 = 0$ and $\alpha_\perp = 6$. It is worth pointing out that this assumption excludes the appearance of instability mechanisms due to the cell shape: for example, rod-like swimming cells in suspension may yield the instability proposed by e.g. [27] and [36]. However, we should also point out that, in many practical situations, this is not a great limitation, as typical gyrotactic cells are often close to a spherical shape (especially *Volvox*). We also note that the sedimentation speed of the cell $V_s^*$ is explicitly included, as it appears to be crucial at high shear rates.

The probability density function is decomposed such that $\Psi^*(\mathbf{x}, \mathbf{e}, t) \equiv n^*(\mathbf{x}^*, t^*) f(\mathbf{x}^*, \mathbf{e}, t^*)$ where $f(\mathbf{x}^*, \mathbf{e}, t^*)$ is the probability density function only for the swimming direction of the cell, satisfying

$$\int_{S_e} f(\mathbf{x}^*, \mathbf{e}, t^*)\ d^2\mathbf{e} = 1, \tag{4a}$$

where $S_e$ is surface of a unit sphere on which the $\mathbf{e}$-space is defined. The probability density distribution function $f(\mathbf{x}^*, \mathbf{e}, t^*)$ allows us to calculate a local ensemble average of an arbitrary variable at a given location $\mathbf{x}^*$: for example, the local ensemble average of the swimming direction at a given location $\mathbf{x}^*$ and time $t^*$ is given by

$$\langle \mathbf{e} \rangle(\mathbf{x}^*, t^*) \equiv \int_{S_e} \mathbf{e} f(\mathbf{x}^*, \mathbf{e}, t^*)\ d^2\mathbf{e}. \tag{4b}$$

It is convenient to split (3) into two equations respectively for $n^*$ and $f$. Integrating (3) over $\mathbf{e}$-space yields the equation for $n^*$:

$$\frac{\partial n^*}{\partial t^*} + \nabla \cdot [n^*(\mathbf{u}^* + V_c^* \langle \mathbf{e} \rangle - V_s^* \mathbf{j})] = \nabla^* \cdot (\mathbf{D}_T^* \cdot \nabla^* n^*), \tag{5}$$

where the diffusivity tensor is approximated by the simplified expression given by [33]:

$$\mathbf{D}_T^* = {V_c^*}^2 \tau(\langle \mathbf{ee} \rangle - \langle \mathbf{e} \rangle \langle \mathbf{e} \rangle). \tag{6}$$

Here, $\tau$ is the correlation time of a cell's random walk, which we will set as a constant. However, in principle, it does not need to be independent of shear rate or of the swimming direction $\mathbf{e}$. We now multiply (5) by $f$ and subtract it from (3). Dividing by $n^*$ then yields the equation for $f$:

$$\frac{\partial f}{\partial t^*} + (\mathbf{u}^* \cdot \nabla) f + \nabla_e \cdot \left\{ \frac{1}{2B} [\mathbf{j} - (\mathbf{j} \cdot \mathbf{e})\mathbf{e}] f + \frac{1}{2} \mathbf{\Omega}^* \wedge \mathbf{e} f \right\} = D_R^* {\nabla_e}^2 f. \tag{7}$$

Here, in obtaining (7), the translational transport by swimming and diffusion of cells is neglected as its contribution appears to be very small for the system of interest: i.e. $h \sim O(1\text{cm})$ and $U_0^*/h \sim O(B^{-1})$.

Regarding the equations of motion here, some additional remarks should be made. First, the randomness in the behaviour of the cell is assumed to be modeled only by the translational diffusivity tensor $\mathbf{D}_T^*$ and the rotational diffusivity $D_R^*$. However, the randomness of the real cells exists in various properties (e.g. swimming speed, size, shape, etc). In this respect, this setting itself is essentially *ad hoc*, as also pointed out by [29]. Furthermore, we also assume that the rotational diffusivity $D_R^*$ does not depend on the shear rate. However, this appears not to be true: a recent

experimental study has shown that the rotational diffusivity exhibits a very large value at the shear rate at which a deterministic swimmer would start to tumble [13]. Finally, it should be pointed out that the translational diffusion model (6) with a 'constant' $\tau$ may not be a good approximation particularly when the shear rate is quite large. This issue has been addressed by several recent studies [15, 28, 1, 8], which have proposed that the spatial dispersion of the cells in strong shear flows is better described by the so-called generalised Taylor dispersion theory. We note that, in practice, the difference between the present analysis and Taylor dispersion theory appears in calculating $\mathbf{D}_T^*$. In particular, the expression (6) in the present study requires an experimental measurement of the correlation time scale $\tau$ as in [16] and [42, 43], and such a measurement is not available in the presence of shear. However, it has been found that (6) with constant $\tau$ is not a bad approximation when the shear rate is not very large [8].

- *Non-dimensionalisation*

The governing equations (1), (2), (5), and (7) are non-dimensionalised using the following dimensionless variables:

$$t = \frac{t^* D_V}{h^2},\ \mathbf{x} = \frac{\mathbf{x}^*}{h},\ \mathbf{u} = \frac{\mathbf{u}^* h}{D_V}\ p = \frac{p^* h^2}{\rho \mu D_V},\ n = \frac{n^*}{N},\ V_c = \frac{V_c^* h}{D_V},\ V_s = \frac{V_s^* h}{D_V}, \tag{8}$$

where $D_V = {V_c^*}^2 \tau$ is the scale for the translational diffusivity, and $N = 1/V \int_\Omega n^* dV$ where $\Omega$ is the domain of interest with its volume $V$. The equations of motion in terms of these variables are then given as follows:

$$\nabla \cdot \mathbf{u} = 0. \tag{9a}$$

$$\mathrm{Sc}^{-1} \frac{\partial \mathbf{u}}{\partial t} + \mathrm{Sc}^{-1} (\mathbf{u} \cdot \nabla)\mathbf{u} = -\nabla p + \nabla^2 \mathbf{u} - \mathrm{Ra}\ n\mathbf{j}, \tag{9b}$$

$$\frac{\partial n}{\partial t} + \nabla \cdot [n(\mathbf{u} + V_c \langle \mathbf{e} \rangle - V_s \mathbf{j})] = \nabla \cdot (\mathbf{D}_T \cdot \nabla n), \tag{9c}$$

$$D_R^{-1} \frac{\partial f}{\partial t} + D_R^{-1} (\mathbf{u} \cdot \nabla) f + \nabla_e \cdot [\lambda [\mathbf{j} - (\mathbf{j} \cdot \mathbf{e})\mathbf{e}] f + \frac{1}{2 D_R} \mathbf{\Omega} \wedge \mathbf{e} f] = {\nabla_e}^2 f, \tag{9d}$$

with boundary conditions

$$\mathbf{u}|_{y=\pm 1} = (\pm U_0, 0, 0), \tag{9e}$$

$$[n(\mathbf{u} + V_c \langle \mathbf{e} \rangle - V_s \mathbf{j}) - \mathbf{D}_T \cdot \nabla n]|_{y=\pm 1} \cdot \mathbf{j} = 0, \tag{9f}$$

where

$$\mathrm{Sc} \equiv \frac{\nu}{D_V},\ \mathrm{Ra} \equiv \frac{N v g' h^3}{D_V \nu},\ \mathbf{D}_T = \frac{\mathbf{D}_T^*}{D_V},\ \lambda = \frac{1}{2 B D_R^*},\ D_R \equiv \frac{D_R^* h^2}{D_V}. \tag{9g}$$

Here, Sc is the Schmidt number, Ra, the Rayleigh number, $\mathbf{D}_T$, the dimensionless translational diffusivity tensor, $\lambda$, the dimensionless inverse of the gyrotactic time scale, and $D_R$ is the dimensionless rotational diffusivity. We note that the boundary condition for $n$ imposes zero flux across the walls, which enables the total number of cells to be preserved in time. On the other hand, a boundary condition for $f$ is purposely excluded because the further approximation of (9d) does not allow us to prescribe it. For this reason, we simply assume that (9d) holds even at the walls although this is not technically correct. From this viewpoint, it should be pointed out that prescribing the boundary condition for $f$ might allow one to describe the reported interaction of swimming cells with the solid boundary [22]. However, this issue is beyond the scope of the present study.

- *Basic state*

We calculate a basic state, about which we will add small perturbations. Geometrical homogeneity of the given flow configuration in the streamwise and spanwise directions gives

$$\frac{\partial}{\partial x} = \frac{\partial}{\partial z} = 0, \ \mathbf{u_0} = (\bar{U}, 0, 0). \tag{10}$$

We first rescale the base-flow velocity $\bar{U}$ with the upper-wall velocity, so that the Reynolds number for the given shear is extracted: i.e. $\mathbf{u_0} = (\mathrm{ScRe}\ U, 0, 0)$ where $\mathrm{Re} = U_0^* h/\nu$ is the Reynolds number. The equations for the basic state are then given as

$$\frac{d^2U}{dy^2} = 0, \tag{11a}$$

$$\frac{dP_0}{dy} = -\mathrm{Ra}\ n_0, \tag{11b}$$

$$\Big[V_c\langle e_2\rangle_0 - V_s\Big]\frac{dn_0}{dy} = D_{T0}^{22}\frac{d^2n_0}{dy^2}, \tag{11c}$$

$$\nabla_e \cdot [\lambda[\mathbf{j} - (\mathbf{j}\cdot\mathbf{e})\mathbf{e}]f_0 + \frac{S}{2}\mathbf{\Omega}_0 \wedge \mathbf{e}f_0] = {\nabla_e}^2 f_0, \tag{11d}$$

with boundary conditions,

$$U|_{y=\pm1} = \pm 1, \tag{11e}$$

$$(V_c\langle e_2\rangle_0 - V_s)n_0|_{y=\pm1} - D_{T0}^{22}\frac{dn_0}{dy}|_{y=\pm1} = 0. \tag{11f}$$

Here, $S$ ($\equiv \mathrm{ScRe}/D_R = U_0^*/D_R^* h$) is the dimensionless shear rate normalised by the rotational diffusivity, $P_0$ is the basic-state pressure, and the subscript $_0$ in $\langle e_2\rangle_0$ and $D_{T0}^{22}$ indicates statistical properties obtained with $f_0$. We note that (11d) does not contain any partial derivatives in $\mathbf{x}$ and that it depends only on $\mathbf{e}$. This allows us to solve it separately from the other equations. Once $f_0(\mathbf{e})$ is obtained, it can be used to build the following solutions of (11a) and (11c):

$$U(y) = y, \tag{12a}$$

$$n_0(y) = N_0 e^{\kappa y}, \tag{12b}$$

with

$$N_0 = \frac{\kappa}{\sinh\kappa}, \ \kappa = \frac{V_c\langle e_2\rangle_0 - V_s}{D_T^{22}}. \tag{12c}$$

where $N_0$ is a normalisation constant such that $1/V\int_\Omega n_0 dV = 1$.

- *Linearised equations for small perturbations*

Now, we consider a small perturbation around the basic state:

$$\begin{aligned} &\mathbf{u} = \mathbf{u}_0(\mathbf{x}) + \epsilon\mathbf{u}'(\mathbf{x},t) + O(\epsilon^2), \ p = P_0(\mathbf{x}) + \epsilon p'(\mathbf{x},t) + O(\epsilon^2), \\ &n = n_0(\mathbf{x}) + \epsilon n'(\mathbf{x},t) + O(\epsilon^2), \ f = f_0(\mathbf{e}) + \epsilon f'(\mathbf{x},\mathbf{e},t) + O(\epsilon^2), \end{aligned} \tag{13}$$

where $\mathbf{u}' = (u', v', w')$. The linearised equations of motions are then given as

$$\frac{\partial u'}{\partial x} + \frac{\partial v'}{\partial y} + \frac{\partial w'}{\partial z} = 0, \tag{14a}$$

$$\mathrm{Sc}^{-1}\frac{\partial u'}{\partial t} + \mathrm{Re}\ U\frac{\partial u'}{\partial x} + \mathrm{Re}\ v'\frac{\partial U}{\partial y} = -\frac{\partial p'}{\partial x} + \nabla^2 u', \tag{14b}$$

$$\mathrm{Sc}^{-1}\frac{\partial v'}{\partial t} + \mathrm{Re}\ U\frac{\partial v'}{\partial x} = -\frac{\partial p'}{\partial y} + \nabla^2 v' - \mathrm{Ra}\ n', \tag{14c}$$

$$\mathrm{Sc}^{-1}\frac{\partial w'}{\partial t} + \mathrm{Re}\ U\frac{\partial w'}{\partial x} = -\frac{\partial p'}{\partial z} + \nabla^2 w', \tag{14d}$$

$$\begin{aligned}\frac{\partial n'}{\partial t} &+ \mathrm{ScRe}\ U\frac{\partial n'}{\partial x} + V_c\langle e_1\rangle_0\frac{\partial n'}{\partial x} + (V_c\langle e_2\rangle_0 - V_s)\frac{\partial n'}{\partial y} + V_c\langle e_3\rangle_0\frac{\partial n'}{\partial z}\\ &+ (v' + V_c\langle e_2\rangle')\frac{dn_0}{dy} + V_c n_0\Big(\frac{\partial\langle e_1\rangle'}{\partial x} + \frac{\partial\langle e_2\rangle'}{\partial y} + \frac{\partial\langle e_3\rangle'}{\partial z}\Big)\\ &- \frac{\partial D_T^{12'}}{\partial x}\frac{\partial n_0}{\partial y} - \frac{\partial D_T^{22'}}{\partial y}\frac{\partial n_0}{\partial y} - \frac{\partial D_T^{32'}}{\partial z}\frac{\partial n_0}{\partial y} - D_T^{22'}\frac{d^2 n_0}{dy^2}\\ &- D_{T0}^{11}\frac{\partial^2 n'}{\partial x^2} - 2D_{T0}^{12}\frac{\partial^2 n'}{\partial x\partial y} - D_{T0}^{22}\frac{\partial^2 n'}{\partial y^2} - D_{T0}^{33}\frac{\partial^2 n'}{\partial z^2} = 0.\end{aligned} \tag{14e}$$

$$\begin{aligned}&D_R^{-1}\frac{\partial f'}{\partial t} + S\ U\frac{\partial f'}{\partial x} + \nabla_e\cdot[\lambda[\mathbf{j} - (\mathbf{j}\cdot\mathbf{e})\mathbf{e}]f' + \frac{S}{2}\mathbf{\Omega}_0\wedge\mathbf{e}f'] - {\nabla_e}^2 f'\\ &= -D_R^{-1}\nabla_e\cdot[\frac{1}{2}\mathbf{\Omega}'\wedge\mathbf{e}f_0],\end{aligned} \tag{14f}$$

with boundary conditions

$$u'|_{y=\pm1} = v'|_{y=\pm1} = w'|_{y=\pm1} = 0, \tag{14g}$$

$$[(V_c\langle e_2\rangle_0 - V_s)n' + V_c\langle e_2\rangle' n_0] - D_{T0}^{22}\frac{\partial n'}{\partial y} - D_T^{22'}\frac{dn_0}{dy}|_{y=\pm1} = 0. \tag{14h}$$

Here, the superscript $'$ for $\langle e_i\rangle$ and $D_T^{ij}$ $(i,j=1,2,3)$ indicates the statistical properties obtained with $f'$.

It appears that performing a linear stability analysis directly with (14) is quite difficult as $f'$ is six-dimensional owing to its dependence on $t$, $\mathbf{x}$, and $\mathbf{e}$. A numerical approach evidently requires extremely expensive computational cost. Given the number of parameters in the present system, such an approach would not be feasible in practice. Therefore, some approximations should be made to overcome this difficulty. In the present study, we assume that $f'$ is quasi-steady and quasi-unform, yielding the following equation for $f'$ instead of (14f):

$$\nabla_e\cdot[\lambda[\mathbf{j} - (\mathbf{j}\cdot\mathbf{e})\mathbf{e}]f' + \frac{S}{2}\mathbf{\Omega}_0\wedge\mathbf{e}f'] - {\nabla_e}^2 f' = -\frac{1}{2D_R}\nabla_e\cdot[\mathbf{\Omega}'\wedge\mathbf{e}f_0]. \tag{15}$$

It should be mentioned that this approximation would be strictly valid only if $f'$ is slowly varying in time and space: $f'(t,\mathbf{x},\mathbf{e}) = f'(T,\mathbf{X},\mathbf{e})$ where $T=\delta t$ and $\mathbf{X}=\delta\mathbf{x}$ with $\delta\ll 1$. Therefore, the approximation may not be good when the vortical perturbation $\mathbf{\Omega}'$ carries rapidly varying spatio-temporal fluctuation of high wavenumber or frequency. However, such a vortical perturbation would probably be damped by viscosity, thus the approximation may not significantly disturb the range where the instability appears. We also note that the approximation removes the partial derivatives in $t$ and $\mathbf{x}$ in (14f). Thus, the initial and boundary conditions for these independent variables cannot be set. Also, this approximation makes the present approach practically identical to that in [33].

Under this approximation, the left-hand side of (15) turns out to be linear and depends only on the swimming direction vector $\mathbf{e}$. On the other hand, the right-hand side is simply a linear combination

of $\mathbf{e}$-dependent functions with coefficients $\omega_1'$, $\omega_2'$, and $\omega_3'$ which are respectively the streamwise, wall-normal, and spanwise components of $\mathbf{\Omega}'(=(\omega_1', \omega_2', \omega_3'))$. This suggests that the solution of (15) is written in the following form:

$$f'(\mathbf{x}, \mathbf{e}, t) = \frac{1}{D_R}[\omega_1'(\mathbf{x}, t) f'_{\omega_1}(\mathbf{e}) + \omega_2'(\mathbf{x}, t) f'_{\omega_2}(\mathbf{e}) + \omega_3'(\mathbf{x}, t) f'_{\omega_3}(\mathbf{e})]. \tag{16}$$

Here, $f'_{\omega_i}(\mathbf{e})$ $(i = 1, 2, 3)$ is the solution of (15) depending only on $\mathbf{e}$ when $D_R = 1$, $\omega_i' = 1$, and $\omega_j' = 0$ for $j \neq i$. The solution form (16) implies that $\langle \mathbf{e} \rangle'$ and $\mathbf{D}_T'$ in (14e) are also written as a linear combination of $\omega_i'$. Examining numerical solution of $f'_{\omega_i}(\mathbf{e})$ allows us to write $\langle \mathbf{e} \rangle'$ and $\mathbf{D}_T'$ as follows:

$$\langle \mathbf{e}_1 \rangle' = \frac{\zeta_1}{D_R}\omega_3', \ \langle \mathbf{e}_2 \rangle' = \frac{\zeta_2}{D_R}\omega_3', \ \langle \mathbf{e}_3 \rangle' = \frac{\zeta_3}{D_R}\omega_1' + \frac{\zeta_4}{D_R}\omega_2', \tag{17a}$$

$$D_T^{12\prime} = \frac{\zeta_5}{D_R}\omega_3', \ D_T^{22\prime} = \frac{\zeta_6}{D_R}\omega_3', \ D_T^{32\prime} = \frac{\zeta_7}{D_R}\omega_1' + \frac{\zeta_8}{D_R}\omega_2', \tag{17b}$$

where $\zeta_i$ are essentially obtained from the first- and the second-order moments of $f'_{\omega_i}(\mathbf{e})$, and they are given in (20).

The approximation allows us to consider the following normal-mode solution of (14),

$$\begin{aligned} &v'(x, y, z, t) = \hat{v}(y) e^{i(\alpha x + \beta z - \omega t)} + c.c, \ \eta'(x, y, z, t) = \hat{\eta}(y) e^{i(\alpha x + \beta z - \omega t)} + c.c \\ &n'(x, y, z, t) = \hat{n}(y) e^{i(\alpha x + \beta z - \omega t)} + c.c, \end{aligned} \tag{18}$$

where $\alpha$ and $\beta$ are respectively the streamwise and spanwise wavenumbers, and $\omega$ is the frequency, resulting in the following equations for linear stability:

$$i\omega \begin{pmatrix} \mathrm{Sc}^{-1}(k^2 - \mathcal{D}^2) & 0 & 0 \\ 0 & \mathrm{Sc}^{-1} & 0 \\ 0 & 0 & I \end{pmatrix} \begin{pmatrix} \hat{v} \\ \hat{\eta} \\ \hat{n} \end{pmatrix} = \begin{pmatrix} L_{OS} & 0 & k^2 \mathrm{Ra} \\ i\beta \mathrm{Re} \mathcal{D} U & L_{SQ} & 0 \\ \mathcal{D} n_0 + L_C^v & L_C^\eta & L_C \end{pmatrix} \begin{pmatrix} \hat{v} \\ \hat{\eta} \\ \hat{n} \end{pmatrix}, \tag{19a}$$

where

$$L_{OS} = i\alpha \mathrm{Re} U(k^2 - \mathcal{D}^2) + i\alpha Re \mathcal{D}^2 U + (k^2 - \mathcal{D}^2)^2, \tag{19b}$$

$$L_{SQ} = i\alpha \mathrm{Re} U + (k^2 - \mathcal{D}^2), \tag{19c}$$

$$\begin{aligned} L_C^v &= \Big[ G_1 \Big( \zeta_2 \mathcal{D} n_0 \frac{i\alpha}{k^2} - n_0 (\zeta_1 \frac{\alpha^2}{k^2} - \zeta_2 \mathcal{D} \frac{i\alpha}{k^2} - \zeta_3 \frac{\beta^2}{k^2}) \Big) - G_2 \Big( \zeta_6 \mathcal{D}^2 n_0 \frac{i\alpha}{k^2} \\ &- \zeta_5 \mathcal{D} n_0 \frac{\alpha^2}{k^2} + \zeta_6 \mathcal{D} n_0 \frac{i\alpha}{k^2} \mathcal{D} + \zeta_7 \mathcal{D} n_0 \frac{\beta^2}{k^2} \Big) \Big] (k^2 - \mathcal{D}^2), \end{aligned} \tag{19d}$$

$$\begin{aligned} L_C^\eta &= \Big[ G_1 \Big( \zeta_2 \mathcal{D} n_0 \frac{i\beta}{k^2} - n_0 (\zeta_1 \frac{\alpha\beta}{k^2} - \zeta_2 \mathcal{D} \frac{i\beta}{k^2} + \zeta_3 \frac{\alpha\beta}{k^2}) \Big) - G_2 \Big( \zeta_6 \mathcal{D}^2 n_0 \frac{i\beta}{k^2} + \zeta_5 \mathcal{D} n_0 \frac{\alpha\beta}{k^2} \\ &- \zeta_6 \frac{i\beta}{k^2} \mathcal{D} n_0 \mathcal{D} + \zeta_7 \mathcal{D} n_0 \frac{\alpha\beta}{k^2} \Big) \Big] \mathcal{D} - G_2 \zeta_8 \mathcal{D} n_0 i\beta, \end{aligned} \tag{19e}$$

$$\begin{aligned} L_C &= i\alpha \mathrm{Sc} \mathrm{Re} U + i\alpha V_c \langle e_1 \rangle + (V_c \langle e_2 \rangle - V_s) D + i\beta V_c \langle e_3 \rangle \\ &+ \alpha^2 D_{T0}^{11} - 2i\alpha D_{T0}^{12} \mathcal{D} - D_{T0}^{22} D^2 + \beta^2 D_{T0}^{33}. \end{aligned} \tag{19f}$$

with boundary conditions,

$$\hat{v}|_{y=\pm 1} = \mathcal{D}\hat{v}|_{y=\pm 1} = 0, \ \hat{\eta}|_{y=\pm 1} = 0,$$

| Parameter | Description | Reference Value | Units |
|---|---|---|---|
| $\rho$ | Fluid density | 1 | g/cm$^3$ |
| $g$ | Gravitational acceleration | 980 | cm/s$^2$ |
| $\nu$ | Dynamic viscosity | 0.01 | cm$^2$/s |
| $d(=2h)$ | Depth of suspension | 0.5 | cm |
| $N$ | Cell mean number density | $1\times10^4 \sim 1\times10^8$ | cells/cm$^3$ |
| $\Delta\rho/\rho$ | Relative cell density | 0.05 | – |
| $v$ | Cell volume | $2.1\times10^{-9}$ | cm$^3$ |
| $g'(=g\Delta\rho/\rho)$ | Relative gravity | 49 | cm/s$^2$ |
| $l$ | Center of gravity offset | $10^{-4}$ | cm |
| $\alpha_0$ | Cell geometry constant | 0 | – |
| $\alpha_\perp$ | Cell geometry constant | 6 | – |
| $B$ | gyrotactic time scale | 3.4 | sec |
| $U_0^*/h$ | Shear rate | $0 \sim 0.74$ | 1/s |
| $V_c^*$ | Swimming speed | $6.3\times10^{-3}$ | cm/s |
| $V_s^*$ | Sedimentation speed | $6\times10^{-4}$ | cm/s |
| $\tau$ | Correlation time scale | 5 | s |
| $D_V^*(=V_c^{*2}\tau)$ | Nominal translation cell diffusivity | $1.98\times10^{-4}$ | cm$^2$/s |
| $D_R^*$ | Rotational diffusivity | 0.067 | 1/s |

Table 1: Parameters and their reference values in the present study. Most of the parameters for the cell properties are taken from the data for *C. Nivalis* [33, 3, 30].

$$\Big[(V_c\langle e_2\rangle_0 - V_s - i\alpha D_{T0}^{12})\hat{n} - D_{T0}^{22}\mathcal{D}\hat{n} + (G_1\zeta_2 n_0 - G_2\zeta_6\mathcal{D}n_0)$$
$$\Big(\frac{i\alpha}{k^2}(k^2-\mathcal{D}^2)\hat{v} + \frac{i\beta}{k^2}\mathcal{D}\hat{\eta}\Big)\Big]_{y=\pm1} = 0, \tag{19g}$$

where $G_1$ describes the importance of swimming relative to rotational diffusion, and $G_2$ represents the importance of translational diffusion relative to rotational diffusion. Here, $L_{OS}$ is the Orr-Sommerfeld operator, $L_{SQ}$ the Squire operator, $L_C$ the advection-diffusion operator for the cell number density, $L_C^v$ the coupling operator between $\hat{v}$ and $\hat{n}$, and $L_C^\eta$ the coupling operator between $\hat{\eta}$ and $\hat{n}$. We note that if $G_1 = G_2 = 0$, the form of the linearised equation is identical to that for Rayleigh-Bénard convection with a cross flow [14, 23, 21]. Computation for the linear instability by excluding the operators for $\eta$ (i.e. $L_{SQ}$, $L_C^\eta$ and $i\beta\mathrm{Re}\mathcal{D}U$) show that their contribution is small, as one might have expected from Squire's theorem [10, 39] and the fact that the wall-normal vorticity $\eta'$ in the Squire equation becomes only a passive variable if $L_C^\eta = 0$. However, it should be mentioned that these operators induce large temporal transient growth of the perturbation even for the stable linear system and that they play a crucial role in the disturbance amplification in bypass transition [12, 5, 35] and fully-developed turbulent flows [18]. This instability, which grows algebraically in inviscid flows [12], can be typically analysed by the so-called 'non-modal' stability analysis [39, 40]. However, this mechanism is active only for $Re \geq 20$, at least [39], whereas the Reynolds number in the present study is less than 20 (see table 2). Therefore, this transiently growing instability can be safely neglected.

| Parameter | Description | Reference Value |
|---|---|---|
| Sc | Schmidt number | 50 |
| Ra | Rayleigh number | $10^1 \sim 10^5$ |
| $S$ | Shear rate normalised by $D_R^*$ | $0 \sim 11$ |
| Re | Reynolds number of base-flow shear | $0 \sim 18$ |
| $\lambda$ | gyrotactic time scale normalised by $D_R^*$ | 2.2 |
| $D_R$ | Rotational diffusivity normalised by $D_V^*$ | 21 |

Table 2: Dimensionless parameters and their values in the present study.

**Parameters**

A list of parameters and their reference values are summarised in table 1. As in previous studies [33, 3, 30, e.g.], most of the parameters are taken from the values relevant for *C. Nivalis* except $\alpha_0$ and $\alpha_\perp$, which are set for a spherical cell. We note that the correlation time scale for the translational diffusivity model is chosen as $\tau = 5$s instead of $\tau = 1.3$s used in e.g. [30] because this value was shown to give better agreement with the experimental data [3]. The depth of the suspension and the shear rate are chosen by considering typical conditions for laboratory experiments [11, 7], so that the results can be compared with the experimental data when available. The dimensionless parameters and their reference values are given in table 2.

**Fokker-Planck equation**

- *Basic state*

The solution of the Fokker-Planck equation $f_0(\mathbf{e})$ under uniform shear was extensively discussed in [4]. For $S = 0$, the numerical solution is identical to the analytic solution in [33] ($f_0(\theta) = \lambda/(4\pi \sinh\lambda) e^{\lambda \cos\theta}$), which is symmetric about the $e_2$-axis (figure 2$a$). As the shear rate $S$ increases, the peak location of $f_0(\mathbf{e})$ is tilted in the direction of shear. However, with increasing $S$, the peak value decreases and $f_0(\mathbf{e})$ tends to be distributed more uniformly.

The mean swimming direction vector $\langle \mathbf{e} \rangle_0$ and the diffusivity tensor $\mathbf{D}_{T0}$ are computed using the calculated $f_0(\mathbf{e})$. Figure 3 ($a$) shows the mean swimming direction vector. For $S = 0$, only the vertical component appears, implying that the cells swim only upward in this case. With an increase of $S$, this component of the mean swimming vector gradually decreases. On the other hand, the streamwise component increases until $S \simeq 5$, after which it also decays with shear. We note that the shear rate at which the deterministic swimmer would experience tumbling is $S_c = 4.4$, suggesting that the decay of the streamwise component is probably associated with this. For very large shear rate ($S > 10$), both components become small although the streamwise one is more persistent than the vertical one. The spanwise component is found to be zero for all $S$ as is to be expected by symmetry. The diffusivity tensor is also shown in figure 3 ($b$). When the shear rate is small, $\mathbf{D}_{T0}$ generally appears to be highly anisotropic. For $S = 0$, $D_{T0}^{22}$ is smaller than $D_{T0}^{11}$ and $D_{T0}^{33}$, and $D_{T0}^{12} = 0$. With the increase of the shear rate from $S = 0$, $D_{T0}^{22}$ and $D_{T0}^{33}$ increase while $D_{T0}^{11}$ and $D_{T0}^{12}$ decrease. The behaviour of $D_{T0}^{11}$ and $D_{T0}^{12}$ is changed around $S = 3 \sim 5$ similarly to the streamwise component of the mean swimming vector (figure 3$a$). However, $D_{T0}^{22}$ and $D_{T0}^{33}$ monotonically increase with the shear rate. For very large shear rate ($S > 10$), the diffusivity tensor becomes nearly isotropic (i.e. $D_{T0}^{11} \simeq D_{T0}^{22} \simeq D_{T0}^{33}$ and $D_{T0}^{12} \simeq 0$).

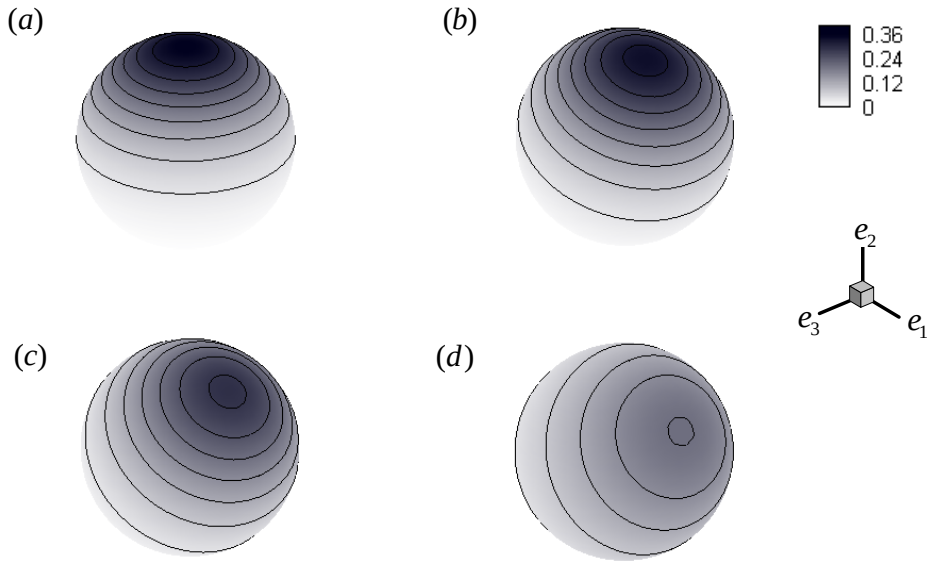


Figure 2: Basic state of probability density function of the cell orientation vector $f_0(\mathbf{e})$ ($\lambda = 2.2$): ($a$) $S = 0$; ($b$) $S = 2$; ($c$) $S = 4$; ($d$) $S = 8$. All the functions exhibit planar symmetry about the $e_1 - e_2$ plane.

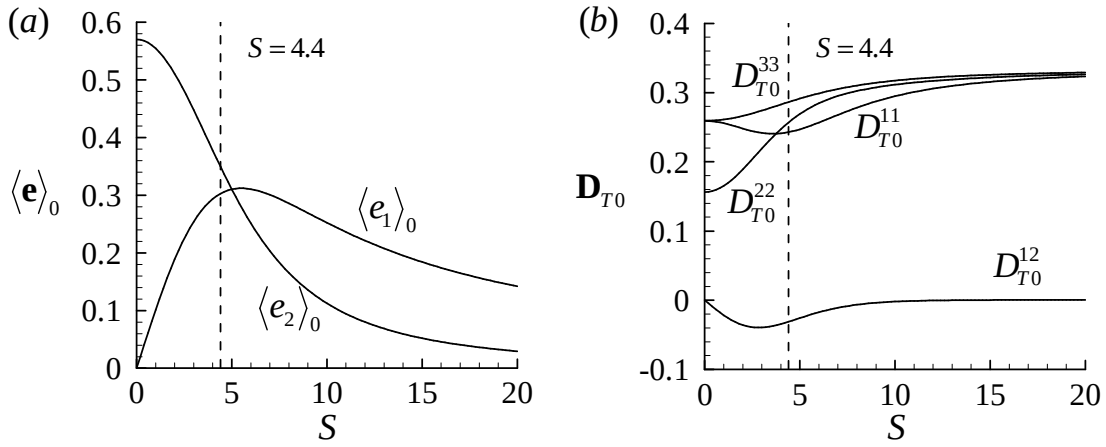


Figure 3: ($a$) Mean cell swimming vector and ($b$) diffusivity tensor ($\lambda = 2.2$). Here, the dashed vertical lines indicate $S = 4.4$ at which the deterministic swimmer begins to experience tumbling. The terms not shown here are zero in numerical precision.

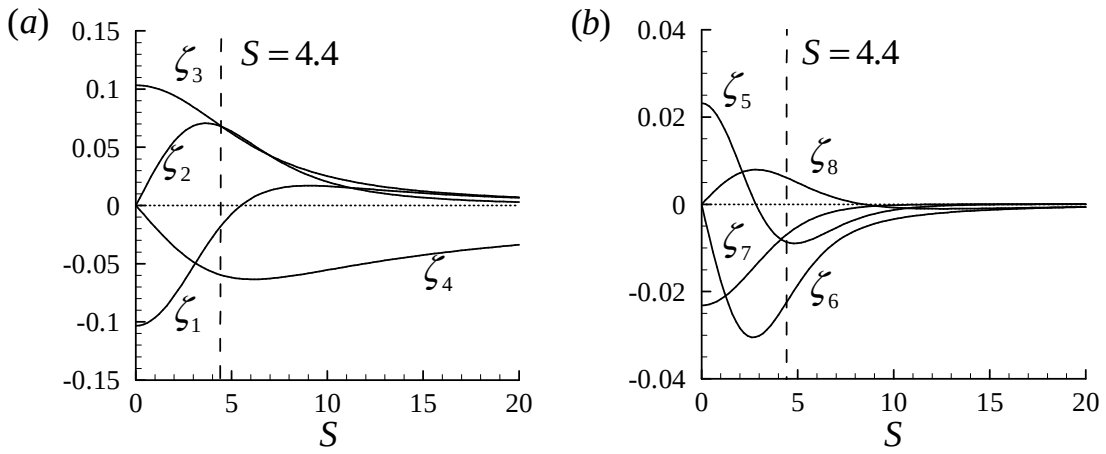


Figure 4: Dependence of $\zeta_i$ on $S$: $(a)$ $\zeta_1$,...,$\zeta_4$; $(b)$ $\zeta_5$,...,$\zeta_8$. Here, the dashed vertical lines indicate $S = 4.4$ at which the deterministic swimmer begins to experience tumbling.

- *Perturbed state*

The perturbed Fokker-Planck equation (15) is also solved, giving the $\zeta_i$'s in (17) as follows:

$$\zeta_1 = \langle e_1\rangle'|_{\omega_3},\ \zeta_2 = \langle e_2\rangle'|_{\omega_3},\ \zeta_3 = \langle e_3\rangle'|_{\omega_1},\ \zeta_3 = \langle e_3\rangle'|_{\omega_2}, \tag{20a}$$

$$\zeta_5 = \langle e_1 e_2\rangle'|_{\omega_3} - \langle e_1\rangle_0\langle e_2\rangle'|_{\omega_3} - \langle e_2\rangle_0\langle e_1\rangle'|_{\omega_3}, \tag{20b}$$

$$\zeta_6 = \langle e_2 e_2\rangle'|_{\omega_3} - 2\langle e_2\rangle_0\langle e_2\rangle'|_{\omega_3}, \tag{20c}$$

$$\zeta_7 = \langle e_3 e_2\rangle'|_{\omega_1} - \langle e_2\rangle_0\langle e_3\rangle'|_{\omega_1}, \tag{20d}$$

$$\zeta_8 = \langle e_3 e_2\rangle'|_{\omega_2} - \langle e_2\rangle_0\langle e_3\rangle'|_{\omega_2}. \tag{20e}$$

The computed $\zeta_i$'s are shown in figure 4.

**Results**

- *Basic state*

To complete the basic state in (12), $\kappa$ should be first calculated from the solution of the Fokker-Planck equation $f_0(\mathbf{e})$. The calculated $\kappa$ is reported in figure 5. For a given depth of suspension, $\kappa$ decreases with the shear rate $S$. This indicates that the cells would accumulate less at the top and that the thickness of the dense cell layer would increase with the shear rate. The decrease of $\kappa$ is not surprising because the mean up-swimming velocity $V_c\langle e_2\rangle_0$ decays with the shear rate (see also figure 3$a$). The decrease is particularly drastic for shear rates less than $S \simeq 4.4$, the value at which a deterministic cell would begin to tumble. For $S \gtrsim 10.9$, $\kappa$ becomes negative because the up-swimming velocity becomes even smaller than the sedimentation velocity ($V_c\langle e_2\rangle_0 < V_s$). Therefore, in this regime, $n_0(y)$ becomes stably stratified. Finally, we note that $\kappa \sim O(h)$ (from (12c) and the non-dimensionalisation (8)): with the increase of the depth, $\kappa$ generally becomes large.

- *Neutral stability curves*

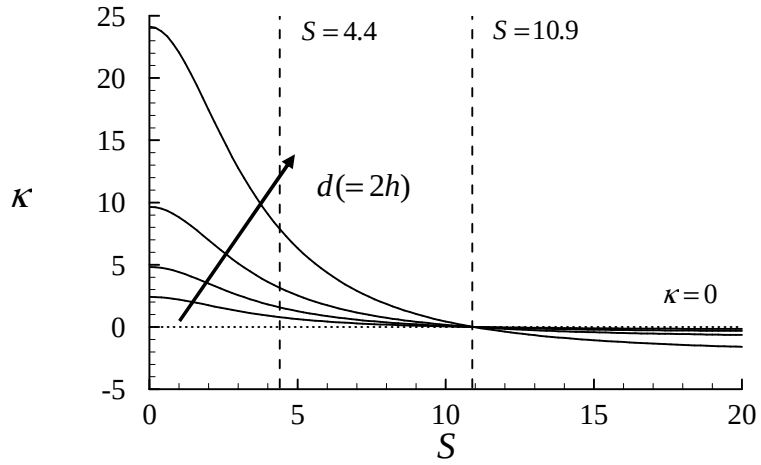


Figure 5: Dependence of the stratification parameter $\kappa$ on the depth of suspension ($d(=2h) = 0.05, 0.1, 0.2, 0.5cm$) and the shear rate $S$. Here, the vertical dashed line in the left indicates the shear rate ($S = 4.4$) at which a deterministic swimmer begins to rumble, while the one in the right is the shear rate ($S = 10.9$) where $\kappa = 0$ due to sedimentation of the swimmer.

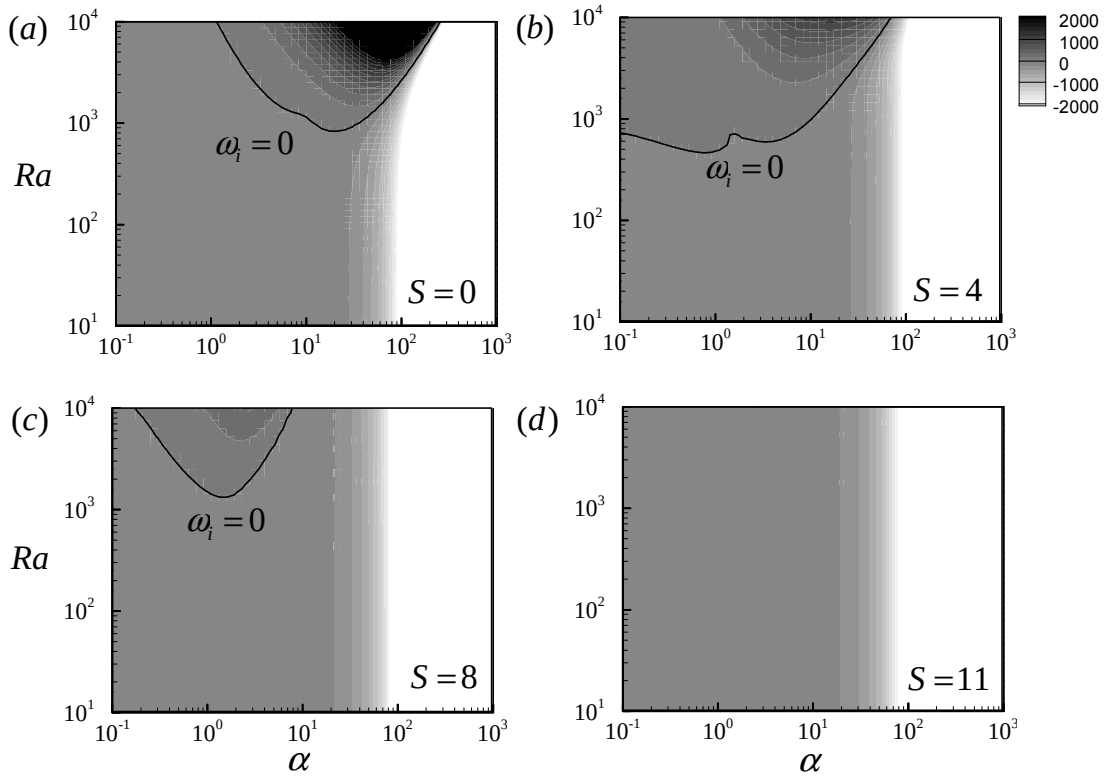


Figure 6: Contour of $\omega_i$ of the most unstable mode and its neutral stability curve in the Ra-$\alpha$ plane for $\alpha \neq 0$ and $\beta = 0$: $(a)$ $S = 0$; $(b)$ $S = 4$; $(c)$ $S = 8$; $(d)$ $S = 11$.

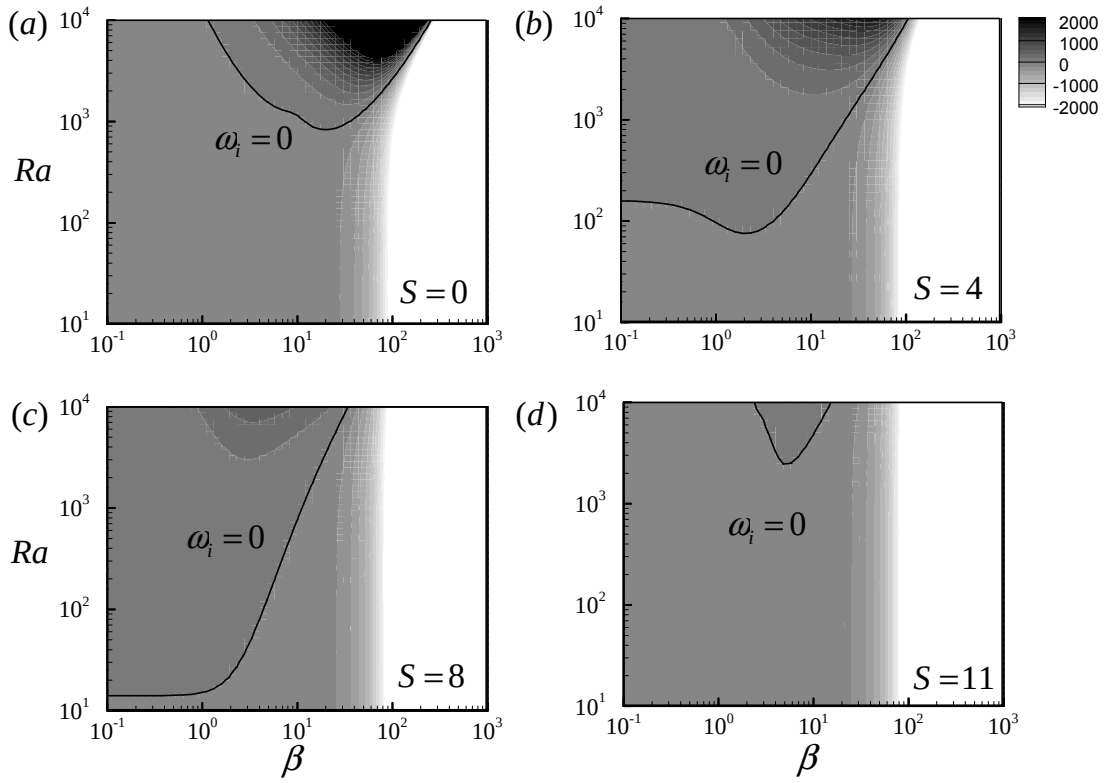


Figure 7: Contour of $\omega_i$ of the most unstable mode and its neutral stability curve in the $Ra$-$\beta$ plane for $\alpha = 0$ and $\beta \neq 0$: $(a)$ $S = 0$; $(b)$ $S = 4$; $(c)$ $S = 8$; $(d)$ $S = 11$.

Linear stability analysis is performed with the reference parameters in tables 1 and 2. We remind the reader that $\alpha$ and $\beta$ are respectively the streamwise and spanwise wavenumbers. We first consider two-dimensional modes (i.e. $\alpha \neq 0$ and $\beta = 0$). Figure 6 shows contours of the growth rate $\omega_i$ and the corresponding neutral stability curve ($\omega_i = 0$) in the Ra-$\alpha$ plane for $S = 0, 4, 8, 11$. Here, note that $S = 11$ gives slightly stable stratification of $n_0(y)$. In the absence of shear ($S = 0$), the instability appears at $\mathrm{Ra}_c \simeq 830$ with the critical wavenumber $\alpha_c \simeq 19$ (figure 6$a$), giving $N_c = 1.05 \times 10^6$ cells/cm$^3$ and $\lambda_c = 0.1$ cm. These values compare reasonably well with $N_c = 1.0 \times 10^6$ cells/cm$^3$ and $\lambda_c = 0.3 \sim 5$ cm in the experiment by [2]. For $S = 0$, the wavenumber giving the largest growth rate tends to increase with Ra, forming strong instability at $\alpha > 20$. However, when shear is introduced, the high-wavenumber instability is drastically damped out (figures 6$b$, $c$, and $d$). In contrast, at relatively low wavenumbers, the shear is destabilising: the suspension is unstable at $\alpha < 1 \sim 10$ even for $Ra \simeq 10^3$ when $S = 4$ and $S = 8$ (figures 6$b$,$c$). For $S = 11$, the instability at small $\alpha$ is stabilised again, thus the suspension does not exhibit instability any more (figure 6$d$).

We now consider the streamwise uniform mode ($\alpha = 0$ and $\beta \neq 0$). The contours of the growth rate $\omega_i$ with the corresponding neutral stability curve in the Ra-$\beta$ plane are shown in figure 7. For $S = 0$, the contour is exactly the same as that in the Ra-$\alpha$ plane (figure 7$a$). Similarly to the two-dimensional mode ($\alpha \neq 0$ and $\beta = 0$), the addition of shear suppresses instability at high wavenumbers ($\beta > 10$), but it augments the instability at low wavenumbers ($\beta < 10$) (figures 7$b$,$c$).

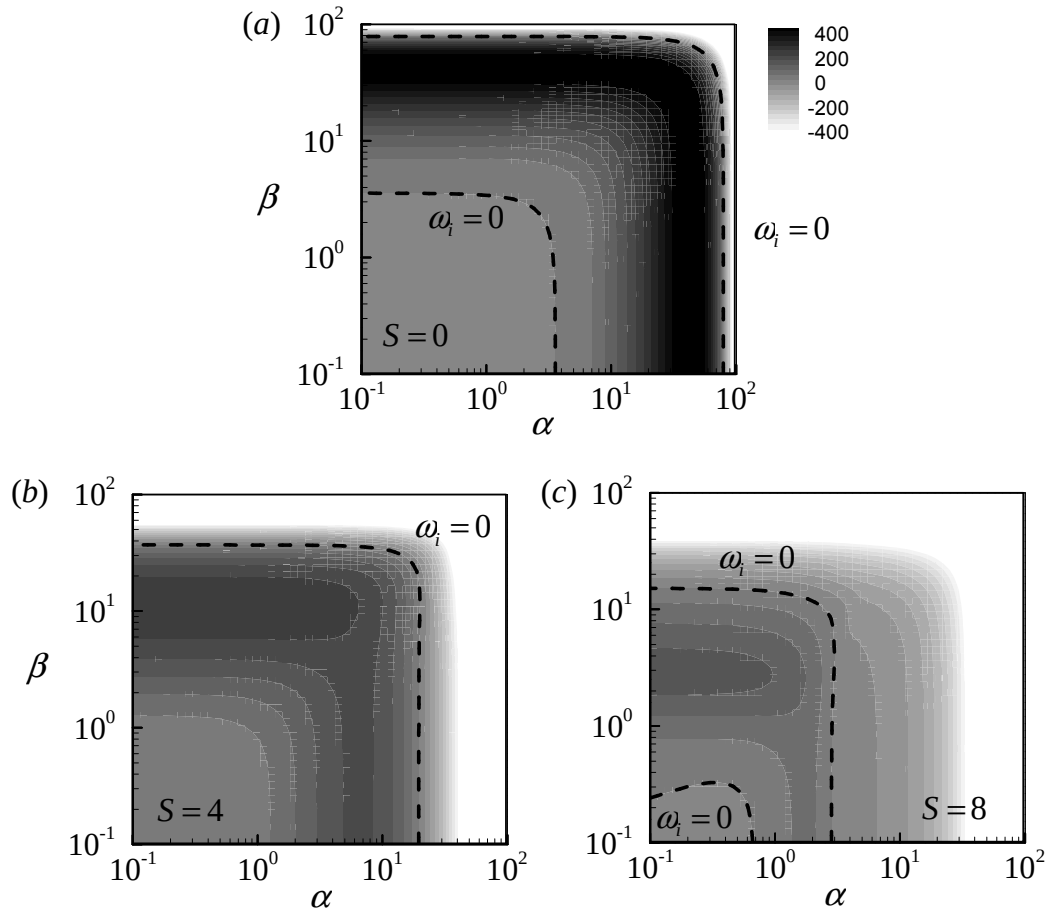


Figure 8: Contour of $\omega_i$ of the most unstable mode and its neutral stability curve for the oblique mode ($\alpha \neq 0$ and $\beta \neq 0$) in the $\alpha$-$\beta$ plane (Ra = 2000): ($a$) $S = 0$; ($b$) $S = 4$; ($c$) $S = 8$.

In particular, the streamwise uniform mode shows much stronger destabilisation than the two-dimensional one, resulting in $\mathrm{Ra}_c \sim O(10)$ for $S = 4$ and $S = 8$. The low-wavenumber instability quickly disappears as soon as the shear rate exceeds $S \simeq 10.9$ which gives stably stratified $n_0(y)$ (figure 7$d$). However, contrary to the two-dimensional mode, the suspension is still linearly unstable at $\beta \simeq 1 \sim 10$, indicating that this instability is not due to the gravitational overturning mechanism.

Finally, oblique modes (i.e. $\alpha \neq 0$ and $\beta \neq 0$) are studied. Figure 8 shows the contours of $\omega_i$ in the $\alpha$-$\beta$ plane at Ra = 2000. As expected, for $S = 0$, the growth rate does not show preference to any specific wavevector directions (figure 8$a$). With the increase of shear rate (e.g. $S = 4$), $\omega_i$ at the high wavenumbers ($\alpha, \beta > 10$) is quickly damped out while that at the low wavenumbers ($\alpha, \beta < 10$) increases a little (figure 8$b$). The further increase of the shear rate ($S = 8$) stabilises the instability at the low wavenumbers ($\alpha, \beta < 10$), similarly to the two-dimensional and streamwise uniform cases. It is interesting to note that the growth rates for $\beta > \alpha$ are generally larger than those for $\alpha > \beta$ in the presence of shear (figures 8$b$ and $c$). In particular, the most unstable set of the two wavenumbers $\alpha$ and $\beta$ appears to be the streamwise uniform mode, indicating that long structures aligned with the shear would appear in the early stages of pattern formation.

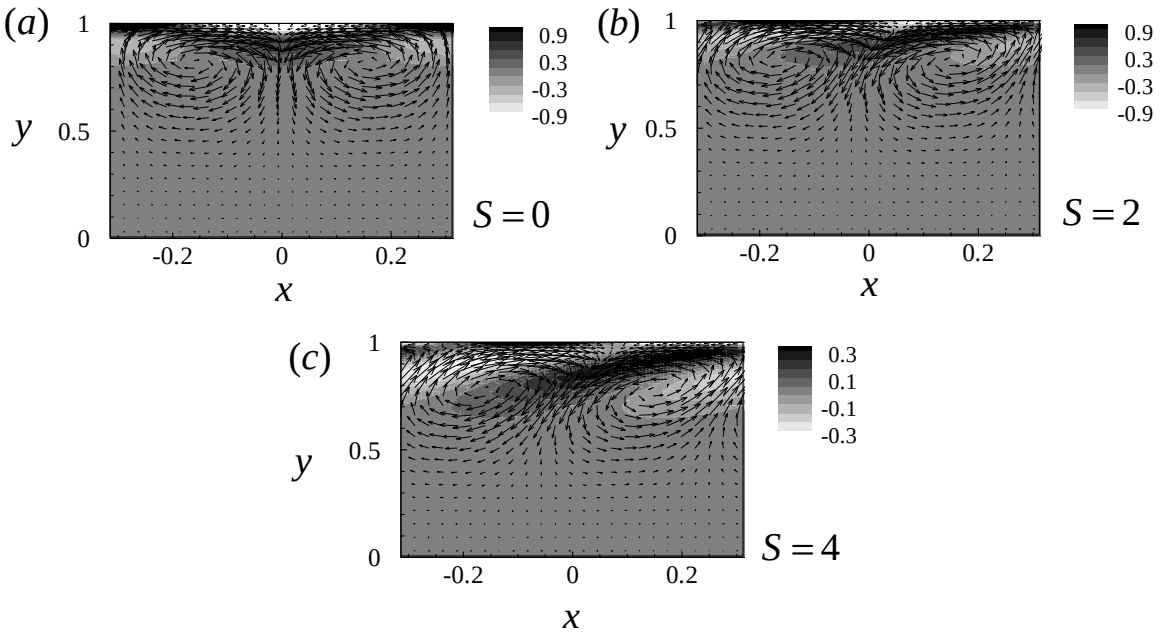


Figure 9: Cross-spanwise view of the eigenfunction for $\alpha = 10$ and $\beta = 0$ at Ra = 2000: $(a)$ $S = 0$; $(b)$ $S = 2$; $(c)$ $S = 4$. Here, the contours represent the perturbed cell number density and the vectors indicate the streamwise and wall-normal velocities. The flow fields are normalized by -$max|\hat{v}|_{x=0}$, so that the downwelling region is located along $x = 0$. Only the upper half is shown due to highly concentrated nature of the eigenfunction near the upper wall.

- *Eigenfunctions*

Figure 9 visualises the eigenfunction of the most unstable two-dimensional mode for increasing shear rate. For $S = 0$, the eigenfunction shows a pair of counter-rotating rolls localised near the top of the domain at which $n_0(y)$ is highly concentrated (figure 9$a$). The cell number density is largest at $x = \pm 0.314$ and $y \simeq 1$, and this is probably due to the rolls which pump up the cells to this region. For this reason, slightly negative $n'$ seems to appear near $x = \pm 0.314$ and $y \simeq 0.9$, which is located right below the region of the largest cell number density. The cell number density $n'$ is smallest at $x = 0$ and $y \simeq 1$ probably because the downflow by the rolls takes the cells in this region to the bottom. Therefore, relatively large $n'$ also appears at the region right below the location with the smallest cell number density ($x = 0$ and $y \simeq 0.9$). When shear is introduced, the entire structure of the eigenfunction is tilted to the shear direction (figure 9$b$). This is evidently due to convective transport by the shear, considering the nature of the shear applied. With the increase of the shear rate $S$, the pattern tilts more downstream (figure 9$c$). It is worth noting that the wall-normal extent occupied by the rolls and the cell number density field appears to increase with the shear rate. This is probably due to the increased thickness of the unstably stratified layer at the top in the basic state: i.e. the decrease of $\kappa$ (figure 5).

The most unstable eigenfunction for the spanwise uniform case is visualised in figure 11. In this case, the eigenfunction does not show the tilting with the increase of $S$, as the convective transport by the shear is perpendicular to the $y$-$z$ plane. The major change by the shear in the eigenfunction structure appears to be the increase of its wall-normal extent. Interestingly, with the increase of the

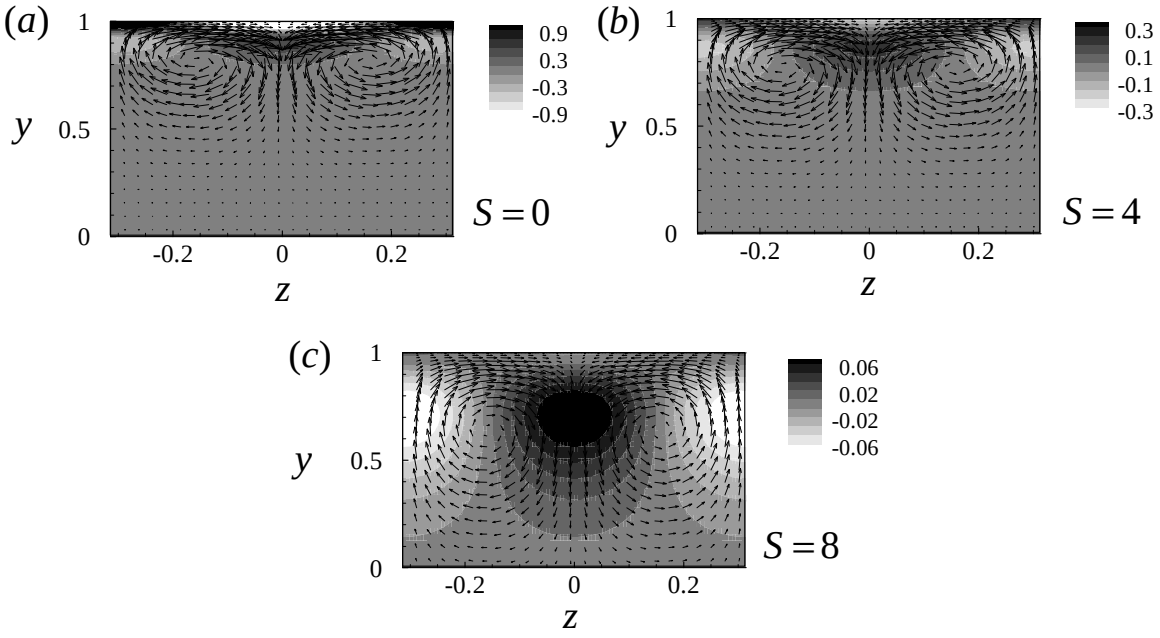


Figure 10: Cross-streamwise view of the eigenfunction for $\alpha = 0$ and $\beta = 10$ at Ra = 2000: ($a$) $S = 0$; ($b$) $S = 4$; ($c$) $S = 8$. Here, the contour represents the perturbed cell number density and the vectors indicate the spanwise and wall-normal velocities. The flow fields are normalized by $-max|v(z = 0)|$. Only the upper half is shown due to highly concentrated nature of the eigenfunction near the upper wall.

shear rate, the location showing the largest (smallest) perturbed cell number density is spontaneously changed to the region where the downward (upward) velocity of the rolls is large (e.g. $y \simeq 0.7$ in figure 11$c$).

## Discussion

- *Comparison with Rayleigh-Bénard convection in uniform shear flow*

Bioconvection patterns have often been compared with those in Rayleigh-Bénard convection because of the remarkable similarity between them. Here, we therefore also aim to compare the role of shear in Rayleigh-Bénard convection with that in bioconvection. In Rayleigh-Bénard convection, the presence of shear stabilises only the streamwise varying modes ($\alpha \neq 0$), leading to the formation of rolls aligned with the shear [23]. Similar shear-aligned rolls are also expected in bioconvection (figure 8), but bioconvective instability exhibits much richer dynamical behaviour than Rayleigh-Bénard convection. First, in bioconvection, the structure of the unstable stratification is highly dependent on the shear rate, as the shear can disturb the up-swimming of individual cells (figure 5). In particular, we have shown that this feature can lead to destabilisation. However, this does not appear in Rayleigh-Bénard convection, as the source of the unstable stratification is the heat flux from the lower wall. Second, bioconvecton in a suspension of bottom-heavy swimmers is caused not only by the gravitational overturning but also by the gyrotaxis of the given swimmer. Specifically, the latter plays an important role in generating instability at high wavenumbers, and this is also found to contribute to the formation of shear-aligned rolls. Lastly, in bioconvection, very strong shear can completely inhibit the instability. However, in Rayleigh-Bénard convection, the shear is not able to control the instability of the streamwise uniform structure because the linearsed equation for the streamwise uniform mode is completely decoupled from the shear [23].

- *Comparison with experimental observations*

In spite of many interesting findings here, there has been limited experimental work to investigate the role of shear in bioconvection. To the best of our knowledge, the only experimental work which allows us to make a comparison is by [7]. In this study, the experimental set-up consists of a horizontal pipe with circular cross section, filled with a suspension of *C. augustae*. To introduce a shear in the suspension, the authors applied a flow through the pipe. The shear rate tested is in a relatively narrow range because it was restricted to be smaller than the value leading to tumbling of a deterministic cell (i.e. $1/B$).

The flow configuration in the present study differs from that in [7], since it is designed to understand the simplest case (i.e. uniform shear). For this reason, only qualitative comparison is made. Since the test section of [7] is circular, it is appropriate to interpret their bioconvection pattern as quasi two-dimensional. Therefore, we only compare the results for the two-dimensional mode ($\alpha \neq 0$ and $\beta = 0$). We have shown that, for a given Rayleigh number (i.e. averaged cell concentration $N$), the increase of shear rate suppresses the instability at high wavenumbers. This yields a decrease of the wavenumber for the largest growth rate, implying that the wavelength of the most unstable two-dimensional mode increases with the shear rate (figure 8). This is seen to be consistent with the experimental observation, where the average spacing between elements of the pattern is shown to increase with the shear rate. However, it should be pointed out that the wavelength computed in the present study deals only with the initial stage of bioconvection whereas the one in the experiment is measured from the fully developed bioconvection pattern. The structure of the eigenfunctions in the present study shows that the shear tilts the pattern of instability, and this is also observed in the experiment; this is not surprising because it is just a consequence of advection by the shear. Finally,

in [7], the pattern at a low cell concentration showed diminishingly small intensity when the through flow was sufficiently strong. In the present study, we have shown that the shear significantly reduces the growth rate at high wavenumbers while it is destabilising at low wavenumber. We note that the increase in the growth rate by the destabilisation is considerably smaller than the decrease at high wavenumbers. Therefore, the present results suggest that the shear may significantly decrease the intensity of the bioconvection although the convection pattern could persist at shear rates smaller than $O(1/B)$. This also appears to be consistent with the experiment, but care needs to be taken as the present analysis is limited to small perturbations.

## • The potential impact (including the socio-economic impact and the wider societal implications of the project so far) and the main dissemination activities and exploitation of results (not exceeding 10 pages)

### Potential impact

From a scientific viewpoint, suspension of swimming microorganisms is an important example of active fluids, dynamics and rheological properties of which are remarkably different from any other complex fluids. It often reveals non-trivial pattern formation (e.g. bioconvection as in this project) driven by intrinsic mechanisms at very small Reynolds numbers, at which nonlinearity in the equation of fluid motions plays little role. This is a very active issue throughout the entire fluid mechanics community although most previous studies investigated stationary configurations. The present work is the first theoretical study which investigates the role of shear in bioconvection patterns. Although the present flow configuration is still very simple, the results have suggested that the physical processes, through which the collective dynamics of microswimmers interacts with the surrounding shear, are not trivial to understand and they actually are remarkably complicated. This finding therefore opens a number of research issues to be studied in the future:

1. How do the physical mechanisms leading to the collective behaviour interact with different types of shear flows such as pressure-driven channel flow, mixing layer, wake and so on?
2. How would the collective dynamics be changed if the direction of gravity relative to flow direction is changed?
3. What if we increase the Reynolds number such that the nonlinear motions created by fluid flow itself interact with the intrinsically driven flow pattern in the microorganism suspension?
4. How is nutrient uptake of microswimmers affected if their collective dynamics is changed by surrounding shear flows?

The issues raised here will be pursued further to attain fundamental understanding of collective dynamics in shear flows, and we believe that this will create a significant impact to scientific communities.

Microorganisms are among the most important life-forms on Earth, not only because of their diversity and cumulative biomass, but also because of their functions in ecosystems. Algal species studied in the present project form the base of the marine food web and produce nearly half of the oxygen produced on earth. They also have socio-economic impact. For example, once a harmful algal bloom occurs, it negatively affects the ecological system in aqueous environment such as freshwater lake and near coastal water. This can create significant economical damage to fishery industry and near-coast recreational facilities. Gaining fundamental understanding of collective behaviour of microorganisms in aqueous environment is very important in this respect. Moreover, this will eventually allow one to develop reliable mathematical models which can predict propagation of algal blooms, thereby reducing the damage caused. This research will therefore create significant socio-economical benefit.

The present project has significant potential importance in designing bioreactors with which biofuel is harvested from cultured microorganisms. The membrane of microorganism, mainly composed of lipid, is processed to oil, and thus the key issue in bioreactor design is to maximize biomass. To culture microorganisms successfully in a bioreactor, nutrient and oxygen should be efficiently delivered to the cells, and this is often achieved through mechanical mixer which generates flow in the

Figure 11: An example of bioreactor

bioreactor. Figure 11 shows an example of a bioreactor. In this type of bioreactor, flow is generated through the pipe lines. Notably, the size of the pipe is not very different from the flow configuration studied in the present project. Although the present project considered the role of uniform shear to gain fundamental understanding of its role, it can certainly be extended to the practical configurations e.g. given in figure 11. In future, a number of important issues will be resolved for developing a reliable mathematical model to predict collective behavior of microorganisms in a bioreactor. Based on this model, a very efficient strategy for mixing will be subsequently developed combining with optimal control theory.

**Dissemination activities and exploitation of results**

Dissemination activities have been performed by publishing papers, attending international and domestic conferences, and giving seminars in a number of academic institutions.

- *Peer reviewed journal publication*

1. Y. Hwang & T. J. Pedley, '*Bioconvection under uniform shear: linear stability analysis*', 2013, To appear *J. Fluid. Mech.*.

2. Y. Hwang, & T. J. Pedley, '*Stability of stationary and downflowing gyrotatic microorganism suspensions in a two-dimensional vertical channel*', 2013, In preparation.

- *Invited Seminar*

1. Oct., 2013, Department of Applied Mathematics and Theoretical Physics (DAMTP), University of Cambridge, Cambridge, UK.

2. July, 2013, Department of Mathematics, University of Manchester, Manchester, UK.

3. June, 2013, Department of Civil and Environmental Engineering, Imperial College, London, UK.

4. Feb., 2013, Department of Mathematics, University of York, UK.

5. Feb., 2013, Department of Mathematics, Imperial College, London, UK.

- *Conference & Workshop*

5. Nov. 2013, 66th Annual Meeting of American Physical Society, Pittsuburgh, US.

4. Sep. 2013, Work shop on Mathematical challenges in bubbles and biological fluid mechanics, Birmingham, UK

3. July 2013, Euromech Colloquium on Trends in open shear flow instability, Paris, France.

2. May 2013, British Applied Mathematics Colloquium, Leeds, UK.

1. Nov. 2012, 65th Annual Meeting of American Physical Society, San Diego, US.

## • The address of the project public website, if applicable as well as relevant contact details

A brief summary of the project and the related publications are found in the following website:

**Website:** http://www3.imperial.ac.uk/people/y.hwang

**Contact details:** Yongyun Hwang, Civil and Environmental Engineering, Imperial College London

**E-mail:** y.hwang@imperial.ac.uk

**Phone:** +44 (0)20 7594 3495

# References


[1] R. N. Bearon, M. A. Bees, and O. A. Croze. Biased swimming cells do not disperse in pipes as tracers: a population model based on microscale behaviour. *Phys. Fluids*, 24:121902, 2012.

[2] M. A. Bees and N. A. Hill. Wavelengths of bioconvection patterns. *J. Exp. Biol.*, 10:1515–1526, 1997.

[3] M. A. Bees and N. A. Hill. Linear bioconvection in a suspension of randomly swimming, gyrotactic micro-organisms. *Phys. Fluid*, 10(8):1864–1881, 1998.

[4] M. A. Bees, N. A. Hill, and T. J. Pedley. Analytical approximations for the orientation distribution of small dipolar particles in steady shear flows. *J. Math. Biol.*, 36:269–298, 1998.

[5] K. M. Butler and B. F. Farrell. Three-dimensional optimal perturbations in viscous shear flow. *Phys. Fluids A*, 4:1637–1650, 1992.

[6] S. Childress, M. Levandowsky, and E. A. Spiegel. Pattern formation in a suspension of swimming micro-organisms. *J. Fluid Mech.*, 69:591–613, 1975.

[7] O. A. Croze, E. E. Ashraf, and M. A. Bees. Sheared bioconvection in a horizontal tube. *Phys. Biol.*, 7:046001, 2010.

[8] O. A. Croze, G. Sardina, M. Ahmed, M. A. Bees, and L. Brandt. Dispersion of swimming algae in laminar and turbulent channel flows: consequences for photobioreactors. *J. Royal Soc. Interface*, 10:20121041, 2013.

[9] C. Dombrowski, B. Lewellyn, A. I. Pesci, J. M. Restrepo, J. O. Kessler, and R. E. Goldstein. Coiling, entrainment, and hydrodynamic coupling of decelerated fluid plumes. *Phys. Rev. Lett.*, 95:184501, 2005.

[10] P.G. Drazin and W.H. Reid. *Hydrodynamic Stability.* Cambridge Univ. Press, 1981.

[11] W. M. Durham, J. O. Kessler, and R. Stocker. Disruption of vertical motility by shear triggers formation of thin phytoplankton layers. *Science*, 323:1067–1070, 2009.

[12] T. Ellingsen and E. Palm. Stability of linear flow. *Phys. Fluids*, 18:487, 1975.

[13] S. Furlan, T. J. Pedley, and R. E. Goldstein. Orientational giant diffusion in gyrotatic microorganisms. 2013. In preparation.

[14] A. P. Gallagher and A. McD. Mercer. On the behavior of small disturbance in plane couette flow with a temperature gradient. *Proc. R. Soc. London.*, 286:117–128, 1965.

[15] N. A. Hill and M. A. Bees. Taylor dispersion of gyrotactic swimming micro-organisms in a linear flow. *Phys. Fluid*, 14:2598–2605, 2002.

[16] N. A. Hill and D.-P. Häder. A biased random walk model for the trajectories of swimming micro-organisms. *J. Theor. Biol.*, 186:503–526, 1997.

[17] N. A. Hill and T. J. Pedley. Bioconvection. *Fluid Dyn. Res.*, 37:1–20, 2005.

[18] Y. Hwang and C. Cossu. Amplification of coherent streaks in the turbulent Couette flow: an input-output analysis at low Reynolds number. *J. Fluid Mech.*, 643:333–348, 2010.

[19] T. Ishikawa. Vertical dispersion of model microorganisms in horizontal shear flow. *J. Fluid Mech.*, 705:98–119, 2012.

[20] G. B. Jeffery. The motion of ellipsoidal particles immersed in a viscous fluid. *Proc. R. Soc. Lond. A*, 102:161–179, 1922.

[21] J. J. S. Jerome, J.-M. Chomaz, and P. Huerre. Transient growth in rayleigh-benard-poiseuille/couette convection. *Phys. Fluids*, 24:044103, 2012.

[22] V. Kantsler, J. Dunkel, M. Polin, and R. E. Goldstein. Ciliary contact interactions dominate surface scattering of swimming eukaryotes. *Proc. Nat. Acad. Sci. USA*, 110:1187–1192, 2013.

[23] J. E. Kelly. The onset and development of thermal convection in fully developed shear flows. *Adv. Appl. Mech*, 31:35–112, 1992.

[24] J. O. Kessler. Gyrotactic buoyant convection and spontaneous pattern formation in algal cell cultures. In M. G. Verlarde, editor, *Non-Equilibrium Cooperative Phenomena in Physics and Related Fields*, pages 241–248. Plenum., 1984.

[25] J. O. Kessler. Hydrodynamics focusing of motile algal cells. *Nature*, 315:218–220, 1985.

[26] J. O. Kessler. Individual and collective dynamics of swimming cells. *J. Fluid Mech.*, 173:191–205, 1986.

[27] D. L. Koch and E. S. G. Shaqfeh. The instability of a dispersion of sedimenting spheroids. *J. Fluid Mech.*, 209:521–541, 1989.

[28] A. Malena and I. Frankel. Generalized taylor dispersion in suspensions of gyrotactic swimming micro-organisms. *J. Fluid Mech.*, 490:99–127, 2003.

[29] T. J. Pedley. Collective behaviour of swimming micro-organisms. *Exp. Mech.*, 50:1293–1301, 2010.

[30] T. J. Pedley. Instability of uniform microorganism suspensions revisited. *J. Fluid Mech.*, 647:335–359, 2010.

[31] T. J. Pedley, N. A. Hill, and J. O. Kessler. The growth of bioconvection patterns in a uniform suspension of gyrotactic micro-organisms. *J. Fluid Mech.*, 195:223–237, 1988.

[32] T. J. Pedley and J. O. Kessler. The orientation of spheroidal microorganisms swimming in a flow field. *Proc. R. Soc. Lond. B*, 231:47–70, 1987.

[33] T. J. Pedley and J. O. Kessler. A new continuum model for suspensions of gyrotactic micro-organisms. *J. Fluid Mech.*, 212:155–182, 1990.

[34] T. J. Pedley and J. O. Kessler. Hydrodynamic phenomena in suspensions of swimming micro-organisms. *Annu. Rev. Fluid Mech.*, 24:313–358, 1992.

[35] S. C. Reddy and D. S. Henningson. Energy growth in viscous channel flows. *J. Fluid Mech.*, 252:209–238, 1993.

[36] D. Saintillan, E. S. G. Shaqfeh, and E. Darve. The growth of concentration fluctuations in dilute dispersions of orientable and deformable particles under sedimentation. *J. Fluid Mech.*, 553:347–388, 2006.

[37] D. Saintillan and M. J. Shelley. Orientiational order and instabilities in suspensions of self-locomoting rods. *Phys. Rev. Lett.*, 99:058102, 2007.

[38] D. Saintillan and M. J. Shelley. Instabilities and pattern formation in active particle suspensions: kinetic theory and continuum simulations. *Phys. Rev. Lett.*, 100:178103, 2008.

[39] P. J. Schmid and D. S. Henningson. *Stability and Transition in Shear Flows.* Springer, New York, 2001.

[40] P.J. Schmid. Nonmodal stability theory. *Annu. Rev. Fluid Mech.*, 39:129–162, 2007.

[41] R. A. Simha and S. Ramaswamy. Hydrodynamic fluctuations and instabilities in ordered suspensions of self-propelled particles. *Phys. Rev. Lett.*, 89:058101, 2002.

[42] V. A. Vladimirov, P. V. Denissenko, T. J. Pedley, M. We, and I. S. Mosklaev. Algal motility measured by a laser based tracking method. *Mar. Freshwater Res.*, 51:589–600, 2000.

[43] V. A. Vladimirov, P. V. Denissenko, T. J. Pedley, M. We, and I. S. Zakhidova. Measurement of cell velocity distributions in populations of motile algae. *J. Exp. Biol*, 207:1203–1216, 2004.

## 4.2 Use and dissemination of foreground

**Section A (public)**

| TEMPLATE A1: LIST OF SCIENTIFIC (PEER REVIEWED) PUBLICATIONS, STARTING WITH THE MOST IMPORTANT ONES | | | | | | | | | | |
|---|---|---|---|---|---|---|---|---|---|---|
| NO. | Title | Main author | Title of the periodical or the series | Number, date or frequency | Publisher | Place of publication | Year of publication | Relevant pages | Permanent identifiers[2] (if available) | Is/Will open access[3] provided to this publication? |
| 1 | *Bioconvection under uniform shear: linear stability anlaysis* | *Y. Hwang & T. J. Pedley* | *Journal of Fluid Mechanics* | *Accepted* | *Cambridge University Press* | *Cambridge* | *?* | | | no |
| 2 | *Stability of a downflowing gyrotactic microorganism suspension in a vertical channel* | *Y. Hwang & T. J. Pedley* | *Journal of Fluid Mechanics* | *In preparation* | *Cambridge University Press* | *Cambridge* | *?* | | | no |

| TEMPLATE A2: LIST OF DISSEMINATION ACTIVITIES |
|---|

[2] A permanent identifier should be a persistent link to the published version full text if open access or abstract if article is pay per view) or to the final manuscript accepted for publication (link to article in repository).

[3] Open Access is defined as free of charge access for anyone via Internet. Please answer "yes" if the open access to the publication is already established and also if the embargo period for open access is not yet over but you intend to establish open access afterwards.

| NO. | Type of activities[4] | Main leader | Title | Date/Period | Place | Type of audience[5] | Size of audience | Countries addressed |
|---|---|---|---|---|---|---|---|---|
| 1 | *Conference* | *Y. Hwang* | *American Physical Society: Annual Meeting in Division of Fluid Dynamics* | *November 2012* | *San Diego, CA* | *Scientific community* | *3000* | US |
| 2 | *Conference* | *Y. Hwang* | *British Applied Mathematics Society:* | *May 2013* | *Leeds* | *Scientific community* | *200* | UK |
| 3 | *Conference* | *Y. Hwang* | *Colloquium of Euromech* | *July 2013* | *Paris* | *Scientific community* | *100* | France |
| 4 | *Workshop* | *Y. Hwang & T. J. Pedley* | *Mathematical challenges in bubbles and biological fluid mechanics* | *September 2013* | *Birmingham* | *Scientific community* | *70* | UK |
| 5 | *Invited Seminar* | *Y. Hwang* | *Mathematics, Imperial College London* | *February 2013* | *London* | *Scientific community* | *50* | UK |
| 6 | *Invited Seminar* | *Y. Hwang* | *Mathematics, University of York* | *February 2013* | *York* | *Scientific community* | *50* | UK |
| 7 | *Invited Seminar* | *Y. Hwang* | *Civil and Environmental Engineering, Imperial College London* | *June 2013* | *London* | *Scientific community* | *50* | UK |
| 8 | *Invited Seminar* | *Y. Hwang* | *Mathematics, University of Manchester* | *July 2013* | *Manchester* | *Scientific community* | *50* | UK |

[4] A drop down list allows choosing the dissemination activity: publications, conferences, workshops, web, press releases, flyers, articles published in the popular press, videos, media briefings, presentations, exhibitions, thesis, interviews, films, TV clips, posters, Other.

[5] A drop down list allows choosing the type of public: Scientific Community (higher education, Research), Industry, Civil Society, Policy makers, Medias, Other ('multiple choices' is possible).

| | | | | | | | | |
|---|---|---|---|---|---|---|---|---|
| 9 | *Private Communication* | *Y. Hwang* | *Schlumberger Gould Research Center* | *May 2013* | *Cambridge* | *Industry* | *30* | UK |

**Section B (Confidential[6] or public: confidential information to be marked clearly)**
**Part B1**

Not applicable to this project.

| TEMPLATE B1: LIST OF APPLICATIONS FOR PATENTS, TRADEMARKS, REGISTERED DESIGNS, ETC. | | | | | |
|---|---|---|---|---|---|
| Type of IP Rights[7]: | Confidential Click on YES/NO | Foreseen embargo date dd/mm/yyyy | Application reference(s) (e.g. EP123456) | Subject or title of application | Applicant (s) (as on the application) |
| | | | | | |
| | | | | | |
| | | | | | |
| | | | | | |

[6] Note to be confused with the "EU CONFIDENTIAL" classification for some security research projects.

[7] A drop down list allows choosing the type of IP rights: Patents, Trademarks, Registered designs, Utility models, Others.

**Part B2**
Please complete the table hereafter:

| Type of Exploitable Foreground[8] | Description of exploitable foreground | Confidential Click on YES/NO | Foreseen embargo date dd/mm/yyyy | Exploitable product(s) or measure(s) | Sector(s) of application[9] | Timetable, commercial or any other use | Patents or other IPR exploitation (licences) | Owner & Other Beneficiary(s) involved |
|---|---|---|---|---|---|---|---|---|
| | | | | | | | | |
| | | | | | | | | |
| | | | | | | | | |

In addition to the table, please provide a text to explain the exploitable foreground, in particular:

- Its purpose
- How the foreground might be exploited, when and by whom
- IPR exploitable measures taken or intended
- Further research necessary, if any
- Potential/expected  impact (quantify where possible)

[19] A drop down list allows choosing the type of foreground: General advancement of knowledge, Commercial exploitation of R&D results, Exploitation of R&D results via standards, exploitation of results through EU policies, exploitation of results through (social) innovation.
[9] A drop down list allows choosing the type sector (NACE nomenclature) : http://ec.europa.eu/competition/mergers/cases/index/nace_all.html

## 4.3 Report on societal implications

Replies to the following questions will assist the Commission to obtain statistics and indicators on societal and socio-economic issues addressed by projects. The questions are arranged in a number of key themes. As well as producing certain statistics, the replies will also help identify those projects that have shown a real engagement with wider societal issues, and thereby identify interesting approaches to these issues and best practices. The replies for individual projects will not be made public.

| **A General Information** *(completed automatically when **Grant Agreement number** is entered.* | |
|---|---|
| **Grant Agreement Number:** | |
| **Title of Project:** | |
| **Name and Title of Coordinator:** | |

| **B Ethics** | |
|---|---|
| **1. Did your project undergo an Ethics Review (and/or Screening)?**<br>• If Yes: have you described the progress of compliance with the relevant Ethics Review/Screening Requirements in the frame of the periodic/final project reports?<br>Special Reminder: the progress of compliance with the Ethics Review/Screening Requirements should be described in the Period/Final Project Reports under the Section 3.2.2 *'Work Progress and Achievements'* | ***0Yes 0No*** |
| **2. Please indicate whether your project involved any of the following issues (tick box) :** | ***No*** |
| **RESEARCH ON HUMANS** | |
| • Did the project involve children? | |
| • Did the project involve patients? | |
| • Did the project involve persons not able to give consent? | |
| • Did the project involve adult healthy volunteers? | |
| • Did the project involve Human genetic material? | |
| • Did the project involve Human biological samples? | |
| • Did the project involve Human data collection? | |
| **RESEARCH ON HUMAN EMBRYO/FOETUS** | |
| • Did the project involve Human Embryos? | |
| • Did the project involve Human Foetal Tissue / Cells? | |
| • Did the project involve Human Embryonic Stem Cells (hESCs)? | |
| • Did the project on human Embryonic Stem Cells involve cells in culture? | |
| • Did the project on human Embryonic Stem Cells involve the derivation of cells from Embryos? | |
| **PRIVACY** | |
| • Did the project involve processing of genetic information or personal data (eg. health, sexual lifestyle, ethnicity, political opinion, religious or philosophical conviction)? | |
| • Did the project involve tracking the location or observation of people? | |
| **RESEARCH ON ANIMALS** | |
| • Did the project involve research on animals? | |
| • Were those animals transgenic small laboratory animals? | |
| • Were those animals transgenic farm animals? | |

| | |
|---|---|
| • Were those animals cloned farm animals? | |
| • Were those animals non-human primates? | |
| **RESEARCH INVOLVING DEVELOPING COUNTRIES** | |
| • Did the project involve the use of local resources (genetic, animal, plant etc)? | |
| • Was the project of benefit to local community (capacity building, access to healthcare, education etc)? | |
| **DUAL USE** | |
| • Research having direct military use | 0 Yes 0 No |
| • Research having the potential for terrorist abuse | |

# C Workforce Statistics

**3. Workforce statistics for the project: Please indicate in the table below the number of people who worked on the project (on a headcount basis).**

| Type of Position | Number of Women | Number of Men |
|---|---|---|
| Scientific Coordinator | 0 | 1 |
| Work package leaders | 0 | 1 |
| Experienced researchers (i.e. PhD holders) | 0 | 1 |
| PhD Students | 0 | 0 |
| Other | 0 | 0 |

| | |
|---|---|
| **4. How many additional researchers (in companies and universities) were recruited specifically for this project?** | **0** |
| Of which, indicate the number of men: | |

## D Gender Aspects

**5. Did you carry out specific Gender Equality Actions under the project**?

○ Yes
○ No

**6. Which of the following actions did you carry out and how effective were they?**

| | Not at all effective | | | | Very effective |
|---|---|---|---|---|---|
| ❑ Design and implement an equal opportunity policy | ○ | ○ | ○ | ○ | ○ |
| ❑ Set targets to achieve a gender balance in the workforce | ○ | ○ | ○ | ○ | ○ |
| ❑ Organise conferences and workshops on gender | ○ | ○ | ○ | ○ | ○ |
| ❑ Actions to improve work-life balance | ○ | ○ | ○ | ○ | ○ |

○ Other:

**7. Was there a gender dimension associated with the research content – i.e. wherever people were the focus of the research as, for example, consumers, users, patients or in trials, was the issue of gender considered and addressed?**

○ Yes- please specify

○ No

## E Synergies with Science Education

**8. Did your project involve working with students and/or school pupils (e.g. open days, participation in science festivals and events, prizes/competitions or joint projects)?**

○ Yes- please specify

○ No

**9. Did the project generate any science education material (e.g. kits, websites, explanatory booklets, DVDs)?**

○ Yes- please specify

○ No

## F Interdisciplinarity

**10. Which disciplines (see list below) are involved in your project?**

○ Main discipline[10]:
○ Associated discipline[10]:
○ Associated discipline[10]:

## G Engaging with Civil society and policy makers

**11a Did your project engage with societal actors beyond the research community?** *(if 'No', go to Question 14)*

○ Yes
○ No

**11b If yes, did you engage with citizens (citizens' panels / juries) or organised civil society (NGOs, patients' groups etc.)?**

○ No
○ Yes- in determining what research should be performed
○ Yes - in implementing the research
○ Yes, in communicating /disseminating / using the results of the project

[10] Insert number from list below (Frascati Manual).

| | | |
|---|---|---|
| **11c In doing so, did your project involve actors whose role is mainly to organise the dialogue with citizens and organised civil society (e.g. professional mediator; communication company, science museums)?** | ○<br>○ | Yes<br>No |

**12. Did you engage with government / public bodies or policy makers (including international organisations)**

- ○ No
- ○ Yes- in framing the research agenda
- ○ Yes - in implementing the research agenda
- ○ Yes, in communicating /disseminating / using the results of the project

**13a Will the project generate outputs (expertise or scientific advice) which could be used by policy makers?**

- ○ Yes – as a **primary** objective (please indicate areas below- multiple answers possible)
- ○ Yes – as a **secondary** objective (please indicate areas below - multiple answer possible)
- ○ No

**13b If Yes, in which fields?**

| | | | | | |
|---|---|---|---|---|---|
| Agriculture | | Energy | | Human rights | |
| Audiovisual and Media | | Enlargement | | Information Society | |
| Budget | | Enterprise | | Institutional affairs | |
| Competition | | Environment | | Internal Market | |
| Consumers | | External Relations | | Justice, freedom and security | |
| Culture | | External Trade | | Public Health | |
| Customs | | Fisheries and Maritime Affairs | | Regional Policy | |
| Development Economic and Monetary Affairs | | Food Safety | | Research and Innovation | |
| | | Foreign and Security Policy | | Space | |
| Education, Training, Youth | | Fraud | | Taxation | |
| Employment and Social Affairs | | Humanitarian aid | | Transport | |

**13c If Yes, at which level?**

- ○ Local / regional levels
- ○ National level
- ○ European level
- ○ International level

## H Use and dissemination

| | |
|---|---|
| **14. How many Articles were published/accepted for publication in peer-reviewed journals?** | **1** |
| **To how many of these is open access[11] provided?** | **0** |
| **How many of these are published in open access journals?** | **0** |
| **How many of these are published in open repositories?** | **0** |
| **To how many of these is open access not provided?** | **1** |
| **Please check all applicable reasons for not providing open access:** | |
| ❑ publisher's licensing agreement would not permit publishing in a repository<br>❑ no suitable repository available<br>❑ no suitable open access journal available<br>❑ no funds available to publish in an open access journal<br>❑ lack of time and resources<br>❑ lack of information on open access<br>❑ other[12]: …… | |

| | | |
|---|---|---|
| **15. How many new patent applications ('priority filings') have been made?** *("Technologically unique": multiple applications for the same invention in different jurisdictions should be counted as just one application of grant).* | | **0** |
| **16. Indicate how many of the following Intellectual Property Rights were applied for (give number in each box).** | Trademark | **0** |
| | Registered design | **0** |
| | Other | **0** |
| **17. How many spin-off companies were created / are planned as a direct result of the project?** | | **0** |
| ***Indicate the approximate number of additional jobs in these companies:*** | | **0** |

**18. Please indicate whether your project has a potential impact on employment, in comparison with the situation before your project:**

| | |
|---|---|
| ❑ Increase in employment, or | ❑ In small & medium-sized enterprises |
| ❑ Safeguard employment, or | ❑ In large companies |
| ❑ Decrease in employment, | ❑ None of the above / not relevant to the project |
| ❑ Difficult to estimate / not possible to quantify | |

| | |
|---|---|
| **19. For your project partnership please estimate the employment effect resulting directly from your participation in Full Time Equivalent (*FTE = one person working fulltime for a year*) jobs:** | *Indicate figure:* |

[11] Open Access is defined as free of charge access for anyone via Internet.
[12] For instance: classification for security project.

| | |
|---|---|
| Difficult to estimate / not possible to quantify | ❑ |

# I Media and Communication to the general public

**20. As part of the project, were any of the beneficiaries professionals in communication or media relations?**

○ Yes ○ No

**21. As part of the project, have any beneficiaries received professional media / communication training / advice to improve communication with the general public?**

○ Yes ○ No

**22 Which of the following have been used to communicate information about your project to the general public, or have resulted from your project?**

| | | | |
|---|---|---|---|
| ❑ | Press Release | ❑ | Coverage in specialist press |
| ❑ | Media briefing | ❑ | Coverage in general (non-specialist) press |
| ❑ | TV coverage / report | ❑ | Coverage in national press |
| ❑ | Radio coverage / report | ❑ | Coverage in international press |
| ❑ | Brochures /posters / flyers | ❑ | Website for the general public / internet |
| ❑ | DVD /Film /Multimedia | ❑ | Event targeting general public (festival, conference, exhibition, science café) |

**23 In which languages are the information products for the general public produced?**

| | | | |
|---|---|---|---|
| ❑ | Language of the coordinator | ❑ | English |
| ❑ | Other language(s) | | |

***Question F-10*:** Classification of Scientific Disciplines according to the Frascati Manual 2002 (Proposed Standard Practice for Surveys on Research and Experimental Development, OECD 2002):

**FIELDS OF SCIENCE AND TECHNOLOGY**

1. NATURAL SCIENCES

1.1 Mathematics and computer sciences [mathematics and other allied fields: computer sciences and other allied subjects (software development only; hardware development should be classified in the engineering fields)]

1.2 Physical sciences (astronomy and space sciences, physics and other allied subjects)

1.3 Chemical sciences (chemistry, other allied subjects)

1.4 Earth and related environmental sciences (geology, geophysics, mineralogy, physical geography and other geosciences, meteorology and other atmospheric sciences including climatic research, oceanography, vulcanology, palaeoecology, other allied sciences)

1.5 Biological sciences (biology, botany, bacteriology, microbiology, zoology, entomology, genetics, biochemistry, biophysics, other allied sciences, excluding clinical and veterinary sciences)

2 ENGINEERING AND TECHNOLOGY

2.1 Civil engineering (architecture engineering, building science and engineering, construction engineering, municipal and structural engineering and other allied subjects)

2.2 Electrical engineering, electronics [electrical engineering, electronics, communication engineering and systems, computer engineering (hardware only) and other allied subjects]

2.3. Other engineering sciences (such as chemical, aeronautical and space, mechanical, metallurgical and materials engineering, and their specialised subdivisions; forest products; applied sciences such as

geodesy, industrial chemistry, etc.; the science and technology of food production; specialised technologies of interdisciplinary fields, e.g. systems analysis, metallurgy, mining, textile technology and other applied subjects)

3. MEDICAL SCIENCES

3.1 Basic medicine (anatomy, cytology, physiology, genetics, pharmacy, pharmacology, toxicology, immunology and immunohaematology, clinical chemistry, clinical microbiology, pathology)

3.2 Clinical medicine (anaesthesiology, paediatrics, obstetrics and gynaecology, internal medicine, surgery, dentistry, neurology, psychiatry, radiology, therapeutics, otorhinolaryngology, ophthalmology)

3.3 Health sciences (public health services, social medicine, hygiene, nursing, epidemiology)

4. AGRICULTURAL SCIENCES

4.1 Agriculture, forestry, fisheries and allied sciences (agronomy, animal husbandry, fisheries, forestry, horticulture, other allied subjects)

4.2 Veterinary medicine

5. SOCIAL SCIENCES

5.1 Psychology

5.2 Economics

5.3 Educational sciences (education and training and other allied subjects)

5.4 Other social sciences [anthropology (social and cultural) and ethnology, demography, geography (human, economic and social), town and country planning, management, law, linguistics, political sciences, sociology, organisation and methods, miscellaneous social sciences and interdisciplinary , methodological and historical S1T activities relating to subjects in this group. Physical anthropology, physical geography and psychophysiology should normally be classified with the natural sciences].

6. HUMANITIES

6.1 History (history, prehistory and history, together with auxiliary historical disciplines such as archaeology, numismatics, palaeography, genealogy, etc.)

6.2 Languages and literature (ancient and modern)

6.3 Other humanities [philosophy (including the history of science and technology) arts, history of art, art criticism, painting, sculpture, musicology, dramatic art excluding artistic "research" of any kind, religion, theology, other fields and subjects pertaining to the humanities, methodological, historical and other S1T activities relating to the subjects in this group]

# 2. FINAL REPORT ON THE DISTRIBUTION OF THE EUROPEAN UNION FINANCIAL CONTRIBUTION

This report shall be submitted to the Commission within 30 days after receipt of the final payment of the European Union financial contribution.

## Report on the distribution of the European Union financial contribution between beneficiaries

| Name of beneficiary | Final amount of EU contribution per beneficiary in Euros |
|---|---|
| 1. | |
| 2. | |
| | |
| n | |
| | |
| Total | |